Article:
Boyd, JL, Riding, JB, Pound, MJ et al. (4 more authors) (2018) The relationship between Neogene dinoflagellate cysts and global climate dynamics. Earth-Science Reviews, 177. pp. 366-385. ISSN 0012-8252

https://doi.org/10.1016/j.earscirev.2017.11.018

The relationship between Neogene dinoflagellate cysts and global climate dynamics

Jamie L. Boyd[1], James B. Riding[2*], Matthew J. Pound[3], Stijn De Schepper[4], Ruza F. Ivanovic[1], Alan M. Haywood[1] and Stephanie E.L. Wood[5]

[1]School of Earth and Environment, University of Leeds, Woodhouse Lane, Leeds LS1 9JT, UK

[2]British Geological Survey, Environmental Science Centre, Keyworth, Nottingham NG12 5GG, UK

*jbri@bgs.ac.uk

[3]Department of Geography and Environmental Sciences, Northumbria University, Newcastle upon Tyne NE1 8ST, UK

[4]Uni Research Climate, Bjerknes Centre for Climate Research, PO Box 7801, N-5020 Bergen, Norway

[5]Department of Animal and Plant Sciences, University of Sheffield, Western Bank, Sheffield S10 2TN, UK

Key Words: dinoflagellate cysts; global distributions; Neogene; palaeoclimate; palaeoecology; palaeotemperature

Abstract

The Neogene Period (23.03–2.58 Ma) underwent a long-term, relatively gradual cooling trend, culminating in the glacial-interglacial climate of the Quaternary. Palaeoclimate studies on the Neogene have provided important information for understanding how modern patterns of atmospheric and oceanic circulation developed, and how they may relate to wider environmental

change. Here we use a newly created global database of Neogene dinoflagellate cysts (the Tertiary Oceanic Parameters Information System - TOPIS) to investigate how dinoflagellate cysts recorded the cooling of Neogene surface marine waters on a global scale. Species with warm and cold water preferences were determined from previously published literature and extracted from the database. Percentages of cold water species were calculated relative to the total number of species with known temperature preferences from each site and compared throughout the Neogene at differing latitudes. Overall, the percentage of cold water species increases gradually through the Neogene. This trend indicates a gradual global cooling that is comparable to that reported from other marine and terrestrial proxies. This also demonstrates the use of dinoflagellate cysts in determining temperature change on both extended temporal and wide geographical scales. The increase in the percentage of cold water species of dinoflagellate cysts recorded worldwide from the Early and Middle Miocene to the Late Pliocene indicates a global scale forcing agent on Neogene climate such as CO_2.

1. Introduction

The Neogene Period (23.03–2.58 Ma) was significantly warmer than the present, and is considered to have been the 'making of the modern world' (Potter and Szatmari, 2009; Pound et al., 2012a) because many important changes occurred that resulted in our current climate. These include alterations to marine gateways (Osbourne et al., 2014; Sijp et al., 2014; Montes et al., 2015), the growth of high latitude continental scale ice sheets (Dowsett et al., 2016; De Schepper et al., 2014; 2015; Brierley and Fedorov, 2016; Stein et al., 2016; Liebrand et al., 2017) and the development of major mountain belts (Raymo and Ruddiman, 1992; Spicer et al., 2003; Graham, 2009; Ruddiman, 2013; von Hagke et al., 2014; Fauquette et al., 2015). All these phenomena combined to change the oceanic and the atmospheric circulations and hence, together with carbon dioxide (CO_2)

47 fluctuations, altered the climate from the relatively warm and ice-free Paleogene, gradually cooling
48 during the Neogene, to the significantly colder temperatures of the Pliocene and Pleistocene
49 (Pearson and Palmer, 2000; Zachos et al., 2001; 2008; Kürschner et al., 2008; Salzmann et al., 2008;
50 2013; Pound et al., 2012a; Herbert et al., 2016; Pound and Salzmann, 2017). The general cooling
51 trend throughout the Cenozoic was occasionally interrupted by several relatively short-lived globally
52 warm intervals. The principal examples of these are the Mid Miocene Climatic Optimum (MMCO)
53 between 17 and 15 Ma (Wright et al., 1992; Flower and Kennett, 1993; 1994; Zachos et al., 2001;
54 2008; Herbert et al., 2016), and the mid Piacenzian Warm Period (mPWP) between 3.264 and 3.025
55 Ma (Haywood et al., 2002; 2013; Robinson et al., 2011). Nevertheless, the longer-term global cooling
56 continued, and eventually culminated in the establishment of large ice sheets in the high northern
57 latitudes (e.g. Shackleton et al. 1984, Jansen et al. 1988, Balco and Rovey 2010) and the decrease of
58 deep sea temperatures by over 10 °C as well as the decrease of surface temperatures of 6 °C (Zachos
59 et al., 2001; 2008; Hansen et al., 2013; Herbert et al., 2016).

60 ## 1.1 Dinoflagellate cysts

61 The paleogeographical distribution of dinoflagellate cysts is increasingly being used to make
62 inferences about palaeoenvironments, including relative temperature estimates (Head, 1994; 1997;
63 Versteegh and Zonneveld, 1994; De Schepper et al., 2009; 2011; 2015; Warny et al., 2009; Schreck
64 and Matthiessen, 2013; Verhoeven and Louwye, 2013; Hennissen et al., 2014). Dinoflagellates are an
65 extant group of unicellular eukaryotic phytoplankton; they are typically marine and planktonic in
66 habit, and are important primary producers (Taylor et al., 2008). Their organic walled resting cysts
67 are most common in marine sediments. Dinoflagellate cysts are normally composed of the
68 biopolymer dinosporin (Fensome et al., 1993; Versteegh et al., 2012; Bogus et al., 2012; 2014),
69 although wall composition differs between taxa, probably related to feeding strategy (Bogus et al.,
70 2014). While the wall of autotrophic dinoflagellate cysts is generally resistant to oxidation,
71 heterotrophic taxa can be degraded and destroyed by oxidation (Zonneveld et al., 1997).

Nevertheless, they are useful proxies for palaeoenvironmental reconstruction because they have global distributions, are abundant and diverse, occur continuously in the fossil record from the mid Triassic onwards and their distribution is controlled by different environmental parameters (Marret and Zonneveld, 2003; Zonneveld et al., 2013). Modern biogeographical distributions are related to parameters such as nutrient levels, salinity, sea ice cover and temperature, although temperature and nutrient availability (phosphate and nitrate concentrations) are thought to be the most important controlling variables (Harland, 1983; Rochon et al., 1999; Marret and Zonneveld, 2003; Radi and de Vernal, 2008; Bonnet et al., 2012; de Vernal et al., 2013; Limoges et al., 2013; Zonneveld et al., 2013a). The environmental preferences of modern dinoflagellate cysts can be compared to the Neogene fossil record of extant taxa, making it possible to infer palaeoenvironmental conditions (Brinkhuis et al., 1998; Sluijs et al., 2005; Masure and Vrielynck, 2009; De Schepper et al., 2011; Woods et al., 2014). However, in deeper time there is an increase in extinct species, which limits the use of the nearest living relative concept (Head, 1996, 1997; Wijnker et al. 2008; De Schepper et al. 2015).

Deciphering the palaeoecology of extinct dinoflagellate cyst species can be achieved by comparing dinoflagellate cyst assemblages with other proxies that provide absolute sea-surface temperatures (De Schepper et al., 2011; Hennissen et al. 2017). These studies have demonstrated that (1) extant species have comparable sea surface temperature ranges in the Pliocene and (2) sea surface temperature ranges can be estimated for extinct species. Other methods include using multivariate analysis to identify temperature-sensitive species (Versteegh, 1994; Hennissen et al. 2017) and determining the latitudinal preferences of species from palaeogeographical maps and inferring a climatological niche from these (Masure and Vrielynck, 2009; Masure et al., 2013).

Due to a limited number of dinoflagellate cyst species with a known absolute temperature range and a lack of abundance data, this study is limited to presenting relative temperature change rather than quantifiable temperatures (Marret and Zonneveld, 2003; Zonneveld et al., 2013a). Species that are

97 constrained to certain temperatures are often regarded as only being abundant in such temperature
98 regimes and rarely outside of them. This means that when using presence and absence data, rather
99 than abundance data, the presence of an individual specimen with cold water preferences does not
100 necessarily rule out warm water conditions. Another example is, in areas of upwelling or river
101 discharge, there is often an increase in the concentration of dinoflagellate cysts due to enhanced
102 nutrient availability (Crouch et al., 2003). Without abundance data, it is difficult to determine the
103 location of upwelling systems and river outlets, and care must be taken to interpret results in light of
104 local phenomenon such as the upwelling of colder, nutrient rich waters.

105 This is the first global study of Neogene marine environmental cooling using dinoflagellate cysts as a
106 temperature proxy. This investigation of an important group of phytoplankton over an interval of
107 >20 Myr provides an unprecedented view of the marine realm worldwide. As such, we are able to
108 answer three key questions: can dinoflagellate cysts be used to determine global cooling in the
109 Neogene? Was the cooling during the Neogene uniform at all latitudes? Was the rate of cooling
110 uniform across the whole Neogene?

111 2. Materials

112 The data used come from the newly developed Tertiary Oceanic Parameters Information System
113 (TOPIS), a Microsoft Access - ArcGIS database containing public domain, peer-reviewed literature on
114 Neogene dinoflagellate cysts. Overall 275 publications are included, totalling 500 globally distributed
115 sites. The database was produced by compiling and entering data from published studies into three
116 forms: 'main', 'layer' and 'flora'. In the 'main' form, key information (bibliographical references,
117 location and approximate age of the samples, dating methods and sample preparation method) is
118 entered with the option to include information on the nearest country and/or ocean basin to the
119 sample site (Figure 1). The 'layer' form contains stratigraphical information such as lithology,
120 formation/member and the detailed age model (Figure 1). This format allows more precise ages to

be given by breaking down the overall cores/outcrop sections into smaller divisions. Therefore, once the third and final form (the 'flora' form) is completed, the dinoflagellate cysts can be shown as part of a smaller and more constrained age range, representing individual assemblages (Figure 1). The 'flora' form documents the individual dinoflagellate cyst taxa and, if available, their relative abundance as a percentage of the total dinoflagellate cyst assemblage (Figure 1). The new database makes it possible to analyse and compare the results of published research on a global scale, and enables global analysis of the development of Neogene oceans and dinoflagellate cyst biogeography over long time scales.

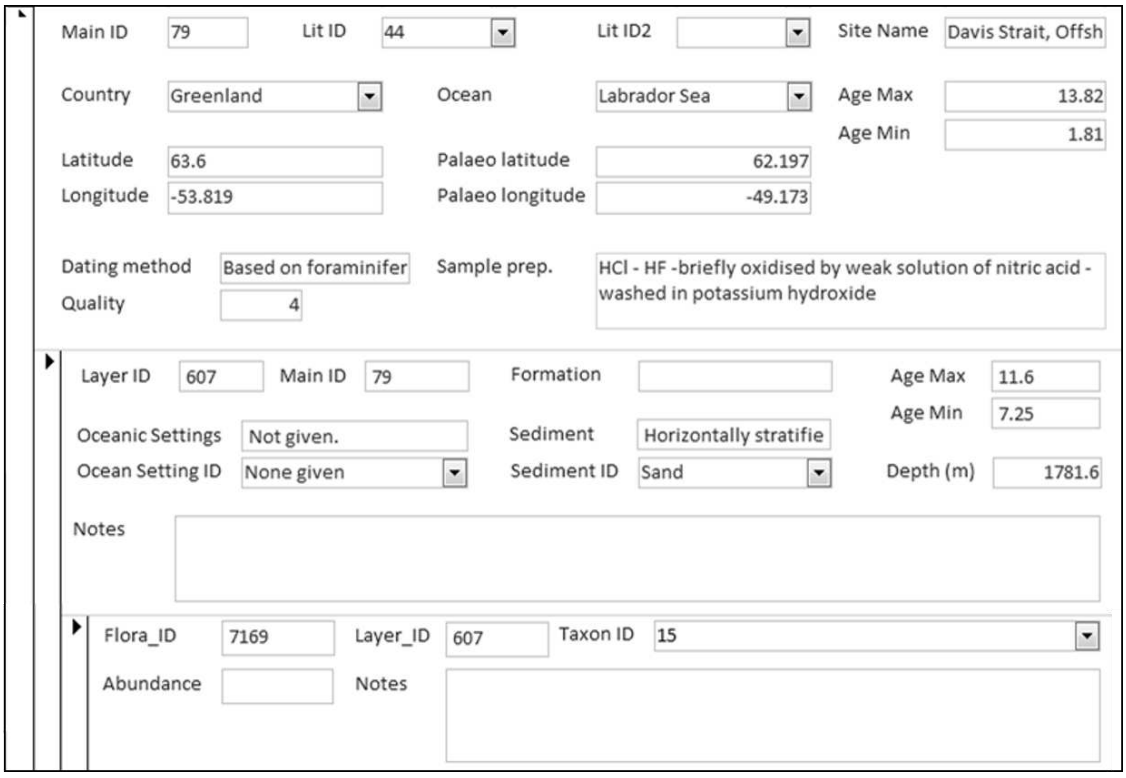

Figure 1: Example screen shot from the Microsoft Access database; Tertiary Oceanic Parameters Information System (TOPIS) showing the three key forms: Main, Layer and Flora.

2.1 Construction of the database

The John Williams Index of Palaeopalynology (JWIP; Riding et al., 2012) was interrogated in order to ensure that the coverage was as comprehensive as possible. The JWIP is the most comprehensive reference catalogue on palaeopalynology in the world, and contains 23,350 references as of

February 2012 (Riding et al., 2012). Whilst it is inevitable that a small amount of literature may have been missed, confidence can be placed in TOPIS to have included the vast majority of available published material on Neogene dinoflagellate cysts. Data published after 2014 have not been included in the analysis in order to facilitate the investigation in a consistent manner.

The diverse nature of the literature used in the TOPIS database means that multiple dating techniques are incorporated into the synthesis. The majority of published dinoflagellate cyst assemblage age assessments were derived biostratigraphically, typically using calcareous nannofossils, foraminifera and palynomorphs, with fewer based on diatoms, mammals, molluscs, magnetostratigraphy or radiometric methods. The dating method in each paper is given a confidence value termed Quality (Figure 1) between one (high) and five (low) in order to estimate the reliability of the dating in a semi-quantitative fashion. In general, studies that utilised multiple dating methods or radiometric dating were assigned Quality values of one or two. Publications using biostratigraphy were assigned a Quality value of either three or four depending on the number of fossil groups used. Whereas, Quality values of five were assigned to publications where only vague dating information was provided.

Because TOPIS contains a diverse range of publications, each with its own different aims and objectives, the resolution of the individual assemblages is variable. Age ranges of individual dinoflagellate cyst assemblages vary from less than 0.001 Myr to over 25 Myr. The majority of the assemblages (1394 assemblages) are dated to within one or two stages of the Neogene and assemblages with a maximum and minimum age range spanning longer than two stages (267 assemblages) were excluded from the analysis to avoid using poorly constrained data that may influence the results. An additional 442 assemblages were included that had estimated age ranges spanning less than one million years. A maximum of two stages were chosen as TOPIS contains assemblages that have a relatively high dating resolution, but happen to span the boundary between two stages.

During the production of this compilation, the date of publication was carefully noted due to the evolving nature of the geological time scale. If the time scale was not explicitly stated in a publication, it was assumed that the most up to date iteration at the time of issue was used. Any changes between pre-2012 versions and Gradstein et al. (2012) were noted. Where necessary, the estimated age ranges of the assemblages were emended to represent the current geological time scale (Gradstein et al., 2012). The majority of the publications affected were those that did not give quantitative age controls, and only provided the stage name(s) as the estimated age range of the assemblages. The major change to the calibration of the Neogene recently was the transition of the Gelasian from the Pliocene into the Pleistocene, effectively shortening the Pliocene to 2.58 Ma (Gibbard et al., 2010). This meant that the age estimates of any publications published prior to 2010, which dated assemblages as Pliocene, were recorded in the database as having an age range of 5.333–1.806 Ma rather than the post-2010 shorter 5.333-2.58 Ma age range of the Pliocene in the modern geological time scale.

Site locations are given as latitude and longitude coordinates, either taken directly from the published literature (when provided), or projected (from the location figure provided) onto a map using online cartographical resources such as Google Earth. If the location was not provided with sufficient resolution, the notes section of the database states that it is approximate. Sites are rotated to their palaeoposition (Figure 2) using a plate rotation model (Pound et al., 2011; Hunter et al., 2013) that is compatible with the underlying palaeogeographies of Markwick et al. (2000).

2.2 Taxonomy, reworking and treatment of dinoflagellate cyst assemblages

The rationale of the TOPIS database follows that of the Tertiary Environmental Vegetation Information System (TEVIS; Salzmann et al., 2008; 2013; Pound et al., 2011; 2012a) and the Bartonian/Rupelian dinoflagellate cyst database of Woods et al. (2014). As in these previously published databases, TOPIS undertakes little reinterpretation of the primary data in order to allow rapid construction and interpretation of large-scale trends (Salzmann et al., 2008; 2013; Pound et al.,

2011; 2012a; Woods et al., 2014). The large amount of data collated, and the broad scale of the analysis, helps mitigate against any problematic taxonomy (Woods et al., 2014).

A consistent dinoflagellate cyst taxonomy based upon Fensome et al. (2008) was used to identify and disregard synonyms. Obvious synonyms were combined/disregarded, and where doubt existed, species were checked against published photographic plates or were not included in any analysis. Synonyms that are combined that are not included in the current version of Dinoflaj2 include: *Barssidinium pliocenicum* and *Barssidinium wrennii* (De Schepper et al., 2004); *Dapsilidinium pseudocolligerum* and *Dapsilidinium pastielsii* (Mertens et al., 2014) and *Operculodinium tegillatum* and *Operculodinium antwerpensis* (Louwye and De Schepper, 2010). These were all recently noted by Williams et al. (2017). Subspecies were treated at the species level; for example, *Achomosphaera andalousiensis* subsp*. andalousiensis* was entered in the database as *Achomosphaera andalousiensis.* Several of the species included in the analysis of this paper have been grouped into complexes (supplementary data A); for example, *Spiniferites elongatus* and *Spiniferites frigidus* have been grouped due to gradations in morphology (Rochon et al., 1999) as were *Batiacasphaera micropapillata* and *Batiacasphaera minuta* (Schreck and Matthiessen, 2013). Taxa not defined to species level and questionably assigned species were also not included in any analysis.

The stratigraphical range for each species in TOPIS was checked, and if reworking of a species was suspected, the species in question was removed from that record. Reworked species were identified by the original authors and/or by checking with previously published range charts produced for the Neogene (e.g. de Verteuil and Norris, 1996; Munsterman and Brinkhuis, 2004; De Schepper and Head, 2008). There is a possibility that some reworked species were still included. However, according to Woods et al. (2014), reworking is unlikely to bias any results due to the large quantity of data analysed, combined with limited evidence of reworking in younger sediments (Mertens et al., 2009; Verleye and Louwye, 2010).

Published dinoflagellate cyst assemblages can be presented as either presence/absence of taxa (e.g. Londeix and Jan du Chene, 1998; Louwye et al., 2000), categorically (e.g. between a range of relative abundances; Head, 1989, McCarthy and Mudie, 1996), as raw abundance counts (e.g. Pudsey and Harland 2001; Louwye et al., 2007) or as relative abundance counts (e.g. Richerol et al., 2012; Shreck et al., 2013). In addition, several different counting techniques were used in the literature compiled herein, for example *Spiniferites* spp. or *Spiniferites*/*Achomosphaera.* Consequently, it was necessary to transform all data into the lowest common form: presence/absence of taxa in order to maximise the geographical and temporal extent of the dataset from TOPIS and to enable identification of large scale trends in dinoflagellate cyst biogeography through the Neogene. Whilst this necessarily loses some of the fine details of abundance variations with regional environmental changes (Marret and Zonneveld, 2003), the focus of this paper is to identify the global scale change.

2.2.1 Preservation/sample preparation technique

The preservation of dinoflagellate cysts can be affected by oxidation, causing decay and poor preservation (de Vernal and Marret, 2007). Oxidation of dinoflagellate cysts can occur naturally and during sample preparation, particularly in older publications, when reagents such as hydrogen peroxide, nitric acid or Schultze's Solution were added to remove residual fine organic material (Riding and Kyffin-Hughes, 2004). Oxidation particularly affects heterotrophic species (e.g. *Brigantedinium* spp.), which are less resistant, and often results in their complete or partial destruction (Marret, 1993; Head, 1996; Zonneveld et al., 1997; 2001; Hopkins and McCarthy, 2002). By contrast, autotrophic species (G-cysts), such as *Impagidinium* spp., are less sensitive to oxidation (Marret and Zonneveld, 2003). This means that the method used for sample preparation must be carefully chosen as some techniques will selectively remove the more oxidation-prone taxa from the assemblage (Marret, 1993; Mudie and McCarthy, 2006).

The distribution of heterotrophic species is mainly controlled by the presence of nutrients, and thus it is likely that both cold and warm water species will be equally affected by any biasing due to

sample preparation methods. If nutrient availability and oxidation are the main controlling influences on the presence and distribution of heterotrophic taxa, rather than temperature (Bockelmann and Zonneveld, 2007), it explains the lack of heterotrophs included amongst the list of species with known temperature preferences (Figure 3 and supplementary data A). Because of these factors, the data compiled herein were not filtered by the sample preparation technique used.

2.2.2 Transport

Dinoflagellate cysts behave as silt sized particles (Dale, 1983; Kawamura, 2004) and, like other microfossil groups, can be transported both vertically through the water column and laterally with ocean currents. This means that there is a possibility that the location at which the fossil was found may not represent the environmental conditions of their original habitat (Dale, 1996; de Vernal and Marret, 2007). Several studies have investigated the effects of vertical and lateral movements of dinoflagellate cysts through the water column by comparing cyst assemblages in the water column to the collection of cysts in the underlying sediments (e.g. Harland and Pudsey, 1999; Zonneveld and Brummer, 2000; Pospelova et al., 2008). These studies indicate that the transport of cysts is only a minor factor in the distribution of cysts and is likely to be a local influence only. Experiments in both laboratories and in the oceans, demonstrate that dinoflagellate cysts sink through the water column relatively rapidly (by several metres per day), which can increase to hundreds of metres per day if they are incorporated into faecal pellets or marine snow (Zonneveld and Brummer, 2000).

In our global scale study, transport does not bias the interpretations. Firstly, transport is a process affecting an entire assemblage, meaning that selective transport of only cool water (or warm water) species is very unlikely. Secondly, the modern biogeographical distribution of cool water species accurately reflects the sea surface temperature distribution in the global oceans (Figure 4i, 4j). Both points, together with the modern observations from sediment traps, suggest that transport in the modern oceans is not a major issue when interpreting the relationship of Cold Water Species (CWS) and Warm Water Species (WWS) in a global dataset.

3. Methods

Dinoflagellates and their cysts make excellent temperature proxies, and as such, numerous publications provide evidence of their temperature preferences (Head, 1997; Marret and Zonneveld, 2003; Wijnker et al., 2008; De Schepper et al., 2009; Schreck et al., 2013; Zonneveld et al., 2013a). The supplementary data (A) presents an updated synthesis of literature from which the temperature preference for each dinoflagellate cyst was obtained. Both modern and palaeontological studies were used to ascertain Neogene dinoflagellate cyst temperature preferences. Temperature categories used in the literature include: tropical, warm-temperate to tropical, temperate, cool-temperate and subpolar, but were simplified in this study into Warm Water Species (WWS) and Cold Water Species (CWS). Our WWS group contains 48 species and includes species within the warm-temperate to tropical categories. The CWS consists of 11 species belonging to the cool-temperate to polar categories (Figure 3; supplementary data A). Sites with any of these species present were extracted from TOPIS for use in this analysis.

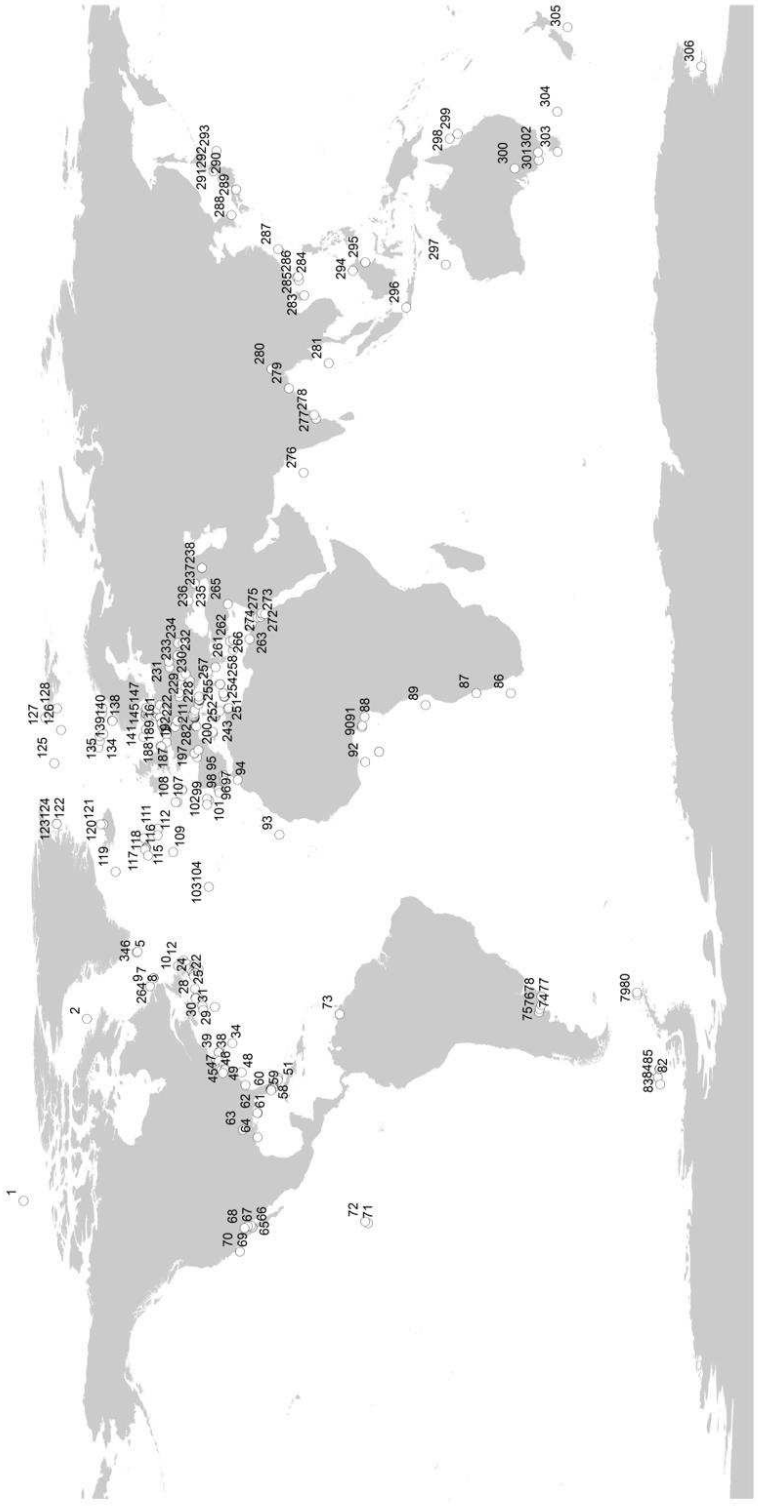

Figure 2: Distribution of all the Neogene records used in this study; the sites are plotted at their modern latitude and longitude, and references are provided in supplementary information B.

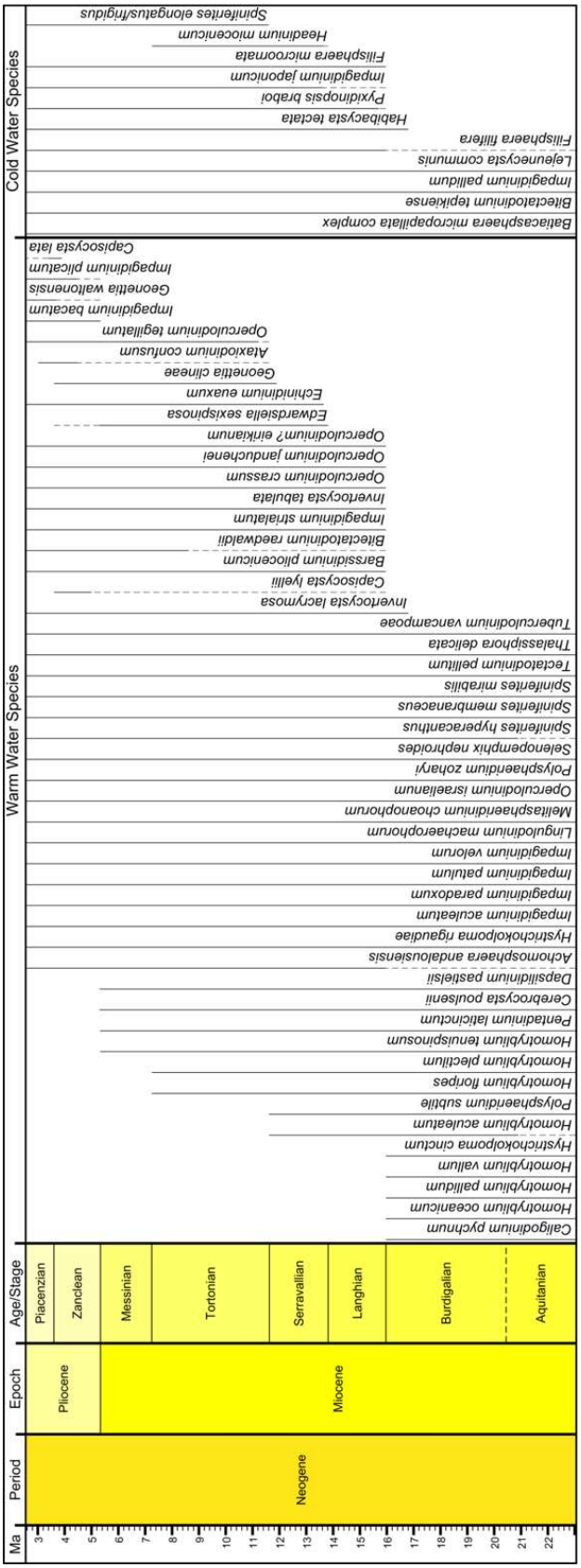

Figure 3: Age ranges of the Neogene dinoflagellate cyst species with known temperature preferences used in this study. Dashed lines represent ages when species are known to have lived, but are not present in the datasets used in this study. References pertaining to temperature preferences are provided in the Supplementary data A.

This resulted in a dataset of 733 records (Figure 2; supplementary data B). The records are from 306 sites (183 publications) and as some sites contain several records of different ages, they have palaeo-latitudes and -longitudes that change through time. A record is defined as one or more dinoflagellate cyst species with a known temperature preference occurring at a location with a specific age range. The percentage of CWS, relative to the total number of species with known temperature preferences in each record, was calculated and plotted in ArcGIS 10.4. For the purposes of plotting the data, records were grouped by geological stage and plotted using their palaeo-latitudes and palaeo-longitudes (Salzmann et al., 2013; Pound et al., 2012a; Pound and Salzmann, 2017). The mean percentage of CWS was calculated for each stage (Figure 6a and b) as well as for each 5° latitudinal bin (Figure 7a-i) to understand the change in surface temperature over the Neogene at different latitudes. As the majority of the data are located in the Northern Hemisphere, much of the analysis ignores the Southern Hemisphere. This is an unfortunate limitation that will be addressed as the literature expands to include more Southern Hemisphere study sites.

Our TOPIS fossil database was compared against the modern dinoflagellate cyst world atlas compiled by Zonneveld et al. (2013b). In the latter database, 33 WWS and 10 CWS were recorded. Seventeen of the WWS and five of the CWS are also found in the Neogene, with the remaining species restricted to the modern or Quaternary oceans. After removing records without known temperature preferences, the modern database was left with a remaining 1,784 records. Cosmopolitan species were considered to have no known temperature preferences as they are not informative for this type of analysis.

4. Results

4.1 Early Miocene (23.03–15.97 Ma)

Only 20% of the records in both the Aquitanian and Burdigalian (Figure 4a, b) had any CWS present, and, with the exception of two records northeast of South America (between 5 and 10° N), no CWS

were found between zero and 25° N (Figures 4a, b, 5). Yet these records off South America contain the highest percentage of CWS relative to WWS in the Northern Hemisphere (25%; *Batiacasphaera micropapillata* complex).

In this study, the *Batiacasphaera micropapillata* complex is defined as a CWS, but they can be found in low quantities at lower latitudes (Schreck and Matthiessen, 2013). This highlights the importance of providing abundance data because without it, it is unclear whether the *B. micropapillata* complex made up a higher percentage of the assemblage (indicating cooler waters), or were present in low abundances.

The highest percentage of CWS in the Southern Hemisphere is between 60 and 65° S, off the Antarctic Peninsula, where two records have CWS percentages of 50 and 100%. Globally, both the Aquitanian and Burdigalian have low mean percentages of 4 and 3% respectively (Figure 6a), although when exclusively using data from the Northern Hemisphere, the mean percentages are 2 and 3% respectively (Figure 6b). The mean percentage of CWS in each five degree latitude bin ranges from zero to 11% for both stages (Figure 7a, b).

4.2 Mid Miocene (15.97–11.62 Ma)

The mean percentage of CWS (relative to WWS) for each five degree latitude bin ranges from zero to 18% for both the Langhian and Serravallian (Figure 7c, d), and globally the mean percentage is 4 and 5% (Figure 6a) respectively (3 and 6% for just the Northern Hemisphere; Figure 6b). The proportion of records with CWS present increased, compared with the Early Miocene (24 and 31% for the Langhian and Serravallian respectively; Figure 4c, d). Unlike in the Aquitanian and Burdigalian, CWS appeared in three records off the east coast of India (10–15° N; *Batiacasphaera micropapillata* complex and *Bitectatodinium tepikiense*) and are also seen in the West Pacific (20%, 35–40° N). Between 40 and 45° N the proportion of CWS increased from mean values of 0.2% in the Burdigalian to 1.8% in the Langhian to 5.3% in the Serravallian (Figure 7b-d). Central Europe in particular

328 experienced an increase in the proportion of CWS relative to WWS during the Mid Miocene (40–55°

329 N; Figures 4c, d, 5a).

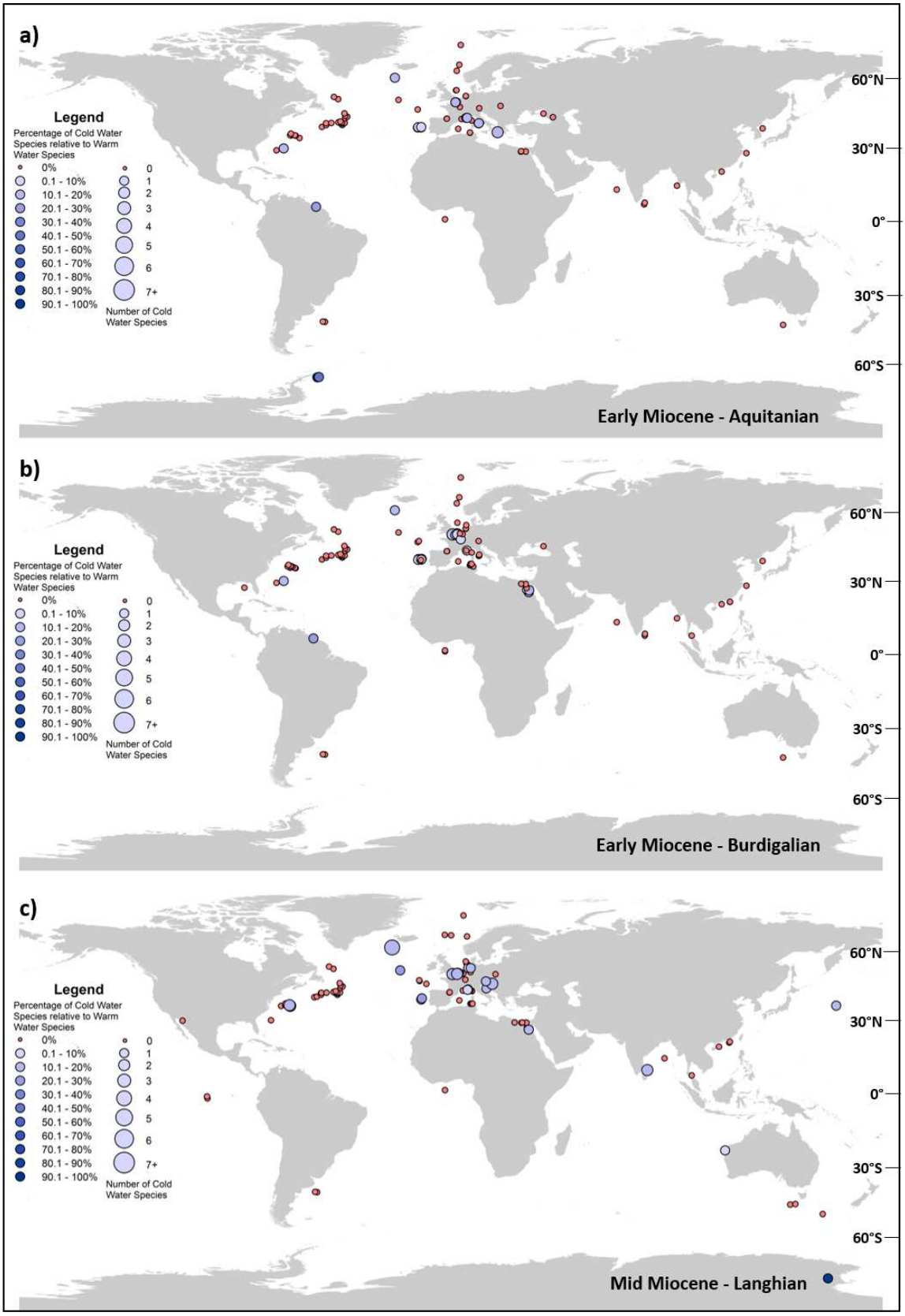
a)
Legend
Percentage of Cold Water Species relative to Warm Water Species
0%
0.1 - 10%
10.1 - 20%
20.1 - 30%
30.1 - 40%
40.1 - 50%
50.1 - 60%
60.1 - 70%
70.1 - 80%
80.1 - 90%
90.1 - 100%
0
1
2
3
4
5
6
7+
Number of Cold Water Species
60°N
30°N
0°
30°S
60°S
Early Miocene - Aquitanian
b)
Legend
Percentage of Cold Water Species relative to Warm Water Species
0%
0.1 - 10%
10.1 - 20%
20.1 - 30%
30.1 - 40%
40.1 - 50%
50.1 - 60%
60.1 - 70%
70.1 - 80%
80.1 - 90%
90.1 - 100%
0
1
2
3
4
5
6
7+
Number of Cold Water Species
60°N
30°N
0°
30°S
60°S
Early Miocene - Burdigalian
c)
Legend
Percentage of Cold Water Species relative to Warm Water Species
0%
0.1 - 10%
10.1 - 20%
20.1 - 30%
30.1 - 40%
40.1 - 50%
50.1 - 60%
60.1 - 70%
70.1 - 80%
80.1 - 90%
90.1 - 100%
0
1
2
3
4
5
6
7+
Number of Cold Water Species
60°N
30°N
0°
30°S
60°S
Mid Miocene - Langhian

330

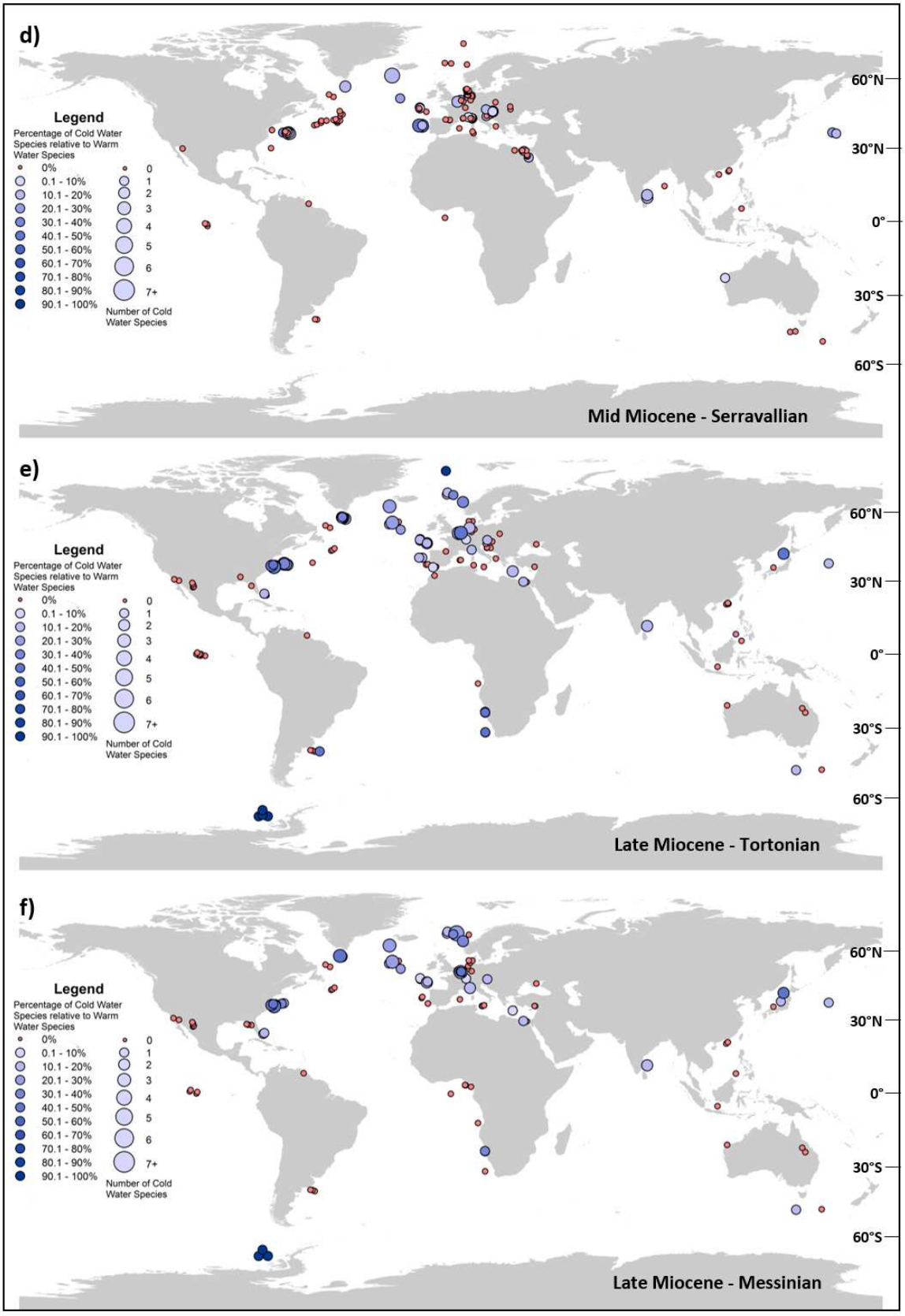
d)
Legend
Percentage of Cold Water Species relative to Warm Water Species
0%
0.1 - 10%
10.1 - 20%
20.1 - 30%
30.1 - 40%
40.1 - 50%
50.1 - 60%
60.1 - 70%
70.1 - 80%
80.1 - 90%
90.1 - 100%
0
1
2
3
4
5
6
7+
Number of Cold Water Species
60°N
30°N
0°
30°S
60°S
Mid Miocene - Serravallian
e)
Legend
Percentage of Cold Water Species relative to Warm Water Species
0%
0.1 - 10%
10.1 - 20%
20.1 - 30%
30.1 - 40%
40.1 - 50%
50.1 - 60%
60.1 - 70%
70.1 - 80%
80.1 - 90%
90.1 - 100%
0
1
2
3
4
5
6
7+
Number of Cold Water Species
60°N
30°N
0°
30°S
60°S
Late Miocene - Tortonian
f)
Legend
Percentage of Cold Water Species relative to Warm Water Species
0%
0.1 - 10%
10.1 - 20%
20.1 - 30%
30.1 - 40%
40.1 - 50%
50.1 - 60%
60.1 - 70%
70.1 - 80%
80.1 - 90%
90.1 - 100%
0
1
2
3
4
5
6
7+
Number of Cold Water Species
60°N
30°N
0°
30°S
60°S
Late Miocene - Messinian

331

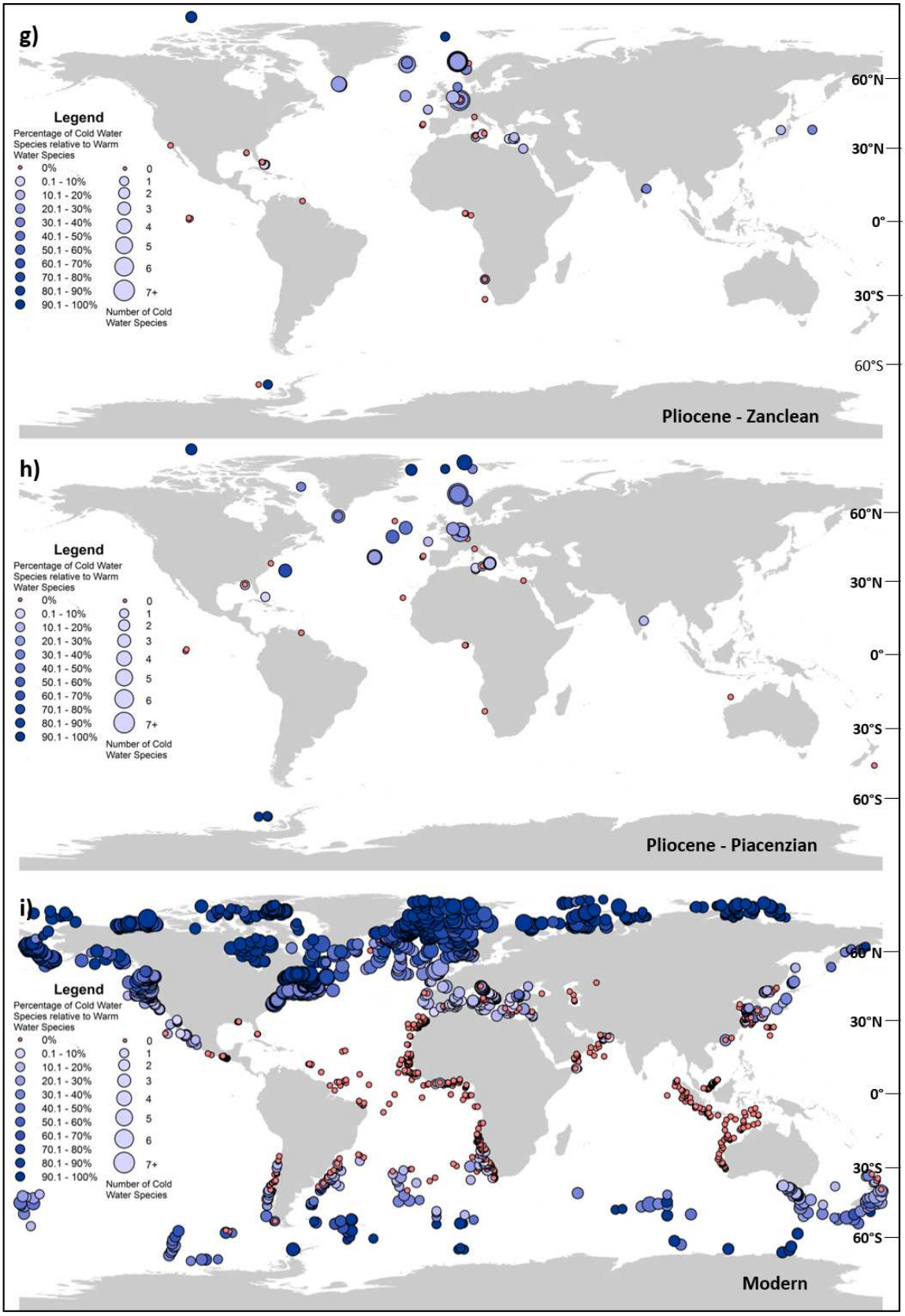
g)
Legend
Percentage of Cold Water Species relative to Warm Water Species
0%
0.1 - 10%
10.1 - 20%
20.1 - 30%
30.1 - 40%
40.1 - 50%
50.1 - 60%
60.1 - 70%
70.1 - 80%
80.1 - 90%
90.1 - 100%
0
1
2
3
4
5
6
7+
Number of Cold Water Species
60°N
30°N
0°
30°S
60°S
Pliocene - Zanclean
h)
Legend
Percentage of Cold Water Species relative to Warm Water Species
0%
0.1 - 10%
10.1 - 20%
20.1 - 30%
30.1 - 40%
40.1 - 50%
50.1 - 60%
60.1 - 70%
70.1 - 80%
80.1 - 90%
90.1 - 100%
0
1
2
3
4
5
6
7+
Number of Cold Water Species
60°N
30°N
0°
30°S
60°S
Pliocene - Piacenzian
i)
Legend
Percentage of Cold Water Species relative to Warm Water Species
0%
0.1 - 10%
10.1 - 20%
20.1 - 30%
30.1 - 40%
40.1 - 50%
50.1 - 60%
60.1 - 70%
70.1 - 80%
80.1 - 90%
90.1 - 100%
0
1
2
3
4
5
6
7+
Number of Cold Water Species
60°N
30°N
0°
30°S
60°S
Modern

332

333

334

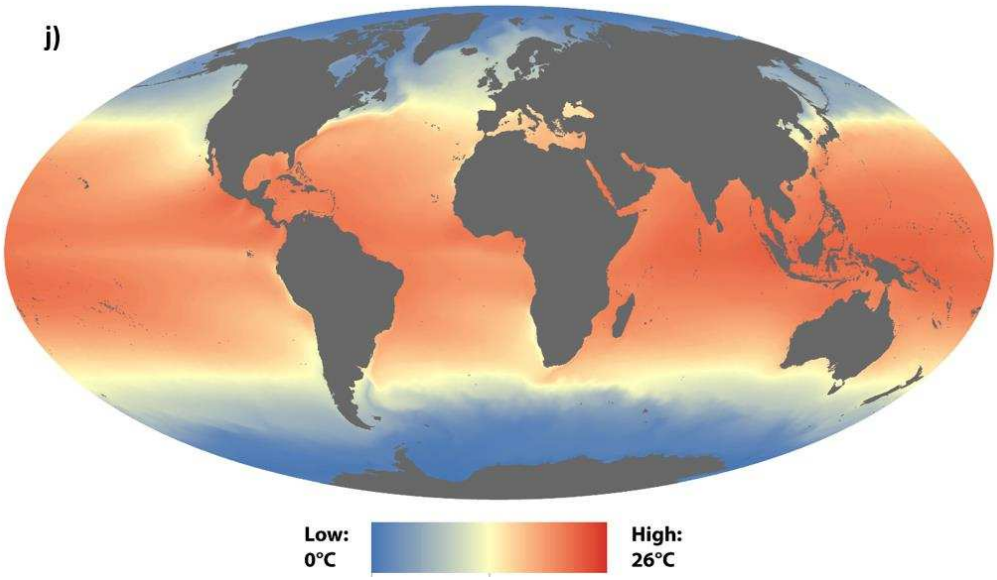

Figure 4: Distribution of dinoflagellate cyst records in (a) Aquitanian, (b) Burdigalian, (c) Langhian, (d) Serravallian, (e) Tortonian, (f) Messinian, (g) Zanclean, (h) Piacenzian and the (i) modern (from Zonneveld et al., 2013b). (j) Mean annual sea surface temperature observed between 2009 and 2013 (from NASA's Ocean Color database: http://oceancolor.gsfc.nasa.gov; NASA Ocean Biology OB.DAAC; 2014). For a-i, records are plotted at their palaeo-latitudes and -longitudes. Size of the points represents the number of Cold Water Species (CWS) present in each record. The colour of the points represents the percentage of CWS relative to the total number of species with known temperature preferences present in each record. Darker shades represent higher percentages of CWS. Small red circles represent records that only contain Warm Water Species.

4.3 Late Miocene (11.62–5.333 Ma)

In the Late Miocene over half of the records contain CWS (Figure 4e, f), and the mean percentage of CWS (relative to WWS) in each latitudinal bin has a much larger range than for the Mid Miocene, between 0 and 27% (Figure 7e, f). One latitudinal bin (in the Tortonian; 75–80° N) is comprised of only CWS (Figures 5a, 7e). Globally the mean percentage of the Tortonian is 19% and the Messinian is 12% (Figure 6a). However, when using just data from the Northern Hemisphere the mean percentage is 11% and 10% for the Tortonian and Messinian respectively (Figure 6b). The high latitudes in particular (50–65° N) had an increase in the proportion of CWS relative to WWS with the introduction of CWS to records off the coast of Norway (up to 33% CWS) and off the coast of Japan (17% CWS; Figure 4e, f). One of the more significant differences between the Tortonian and the rest

354 of the Neogene is the number of records in the Southern Hemisphere, which is substantially higher
355 in the Tortonian than for any of the other stages (Figure 5a). The additional records appear off the
356 Antarctic Peninsula (CWS percentages range from 50 to 100%), and off the west coast of South
357 Africa (CWS percentages of 100%; *Bitectatodinium tepikiense*.

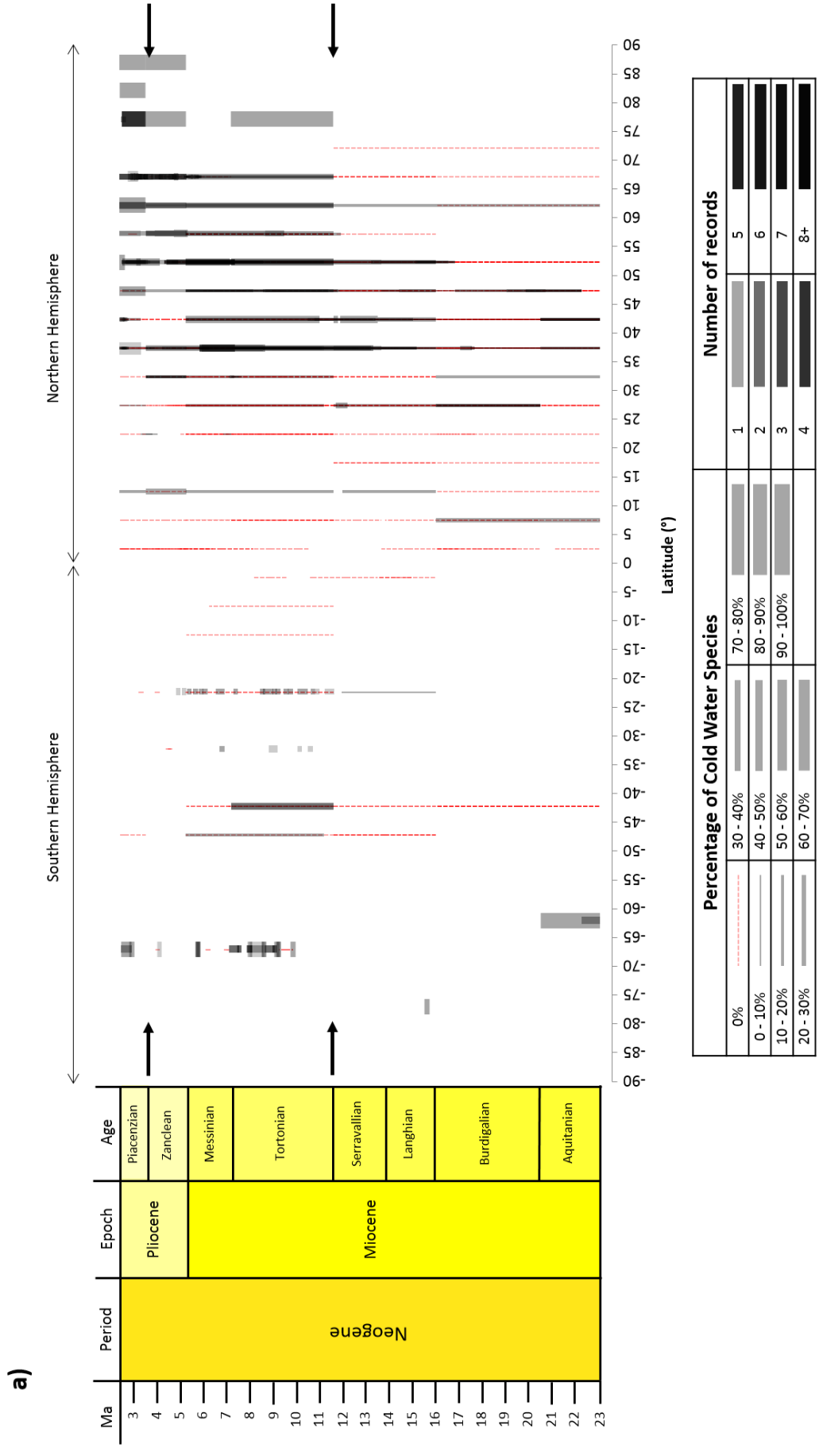
a)
Ma
Period
Epoch
Age
Neogene
Pliocene
Miocene
Piacenzian
Zanclean
Messinian
Tortonian
Serravallian
Langhian
Burdigalian
Aquitanian
Northern Hemisphere
Southern Hemisphere
Latitude (°)
Percentage of Cold Water Species
0%
0 - 10%
10 - 20%
20 - 30%
30 - 40%
40 - 50%
50 - 60%
60 - 70%
70 - 80%
80 - 90%
90 - 100%
Number of records
1
2
3
4
5
6
7
8+

358

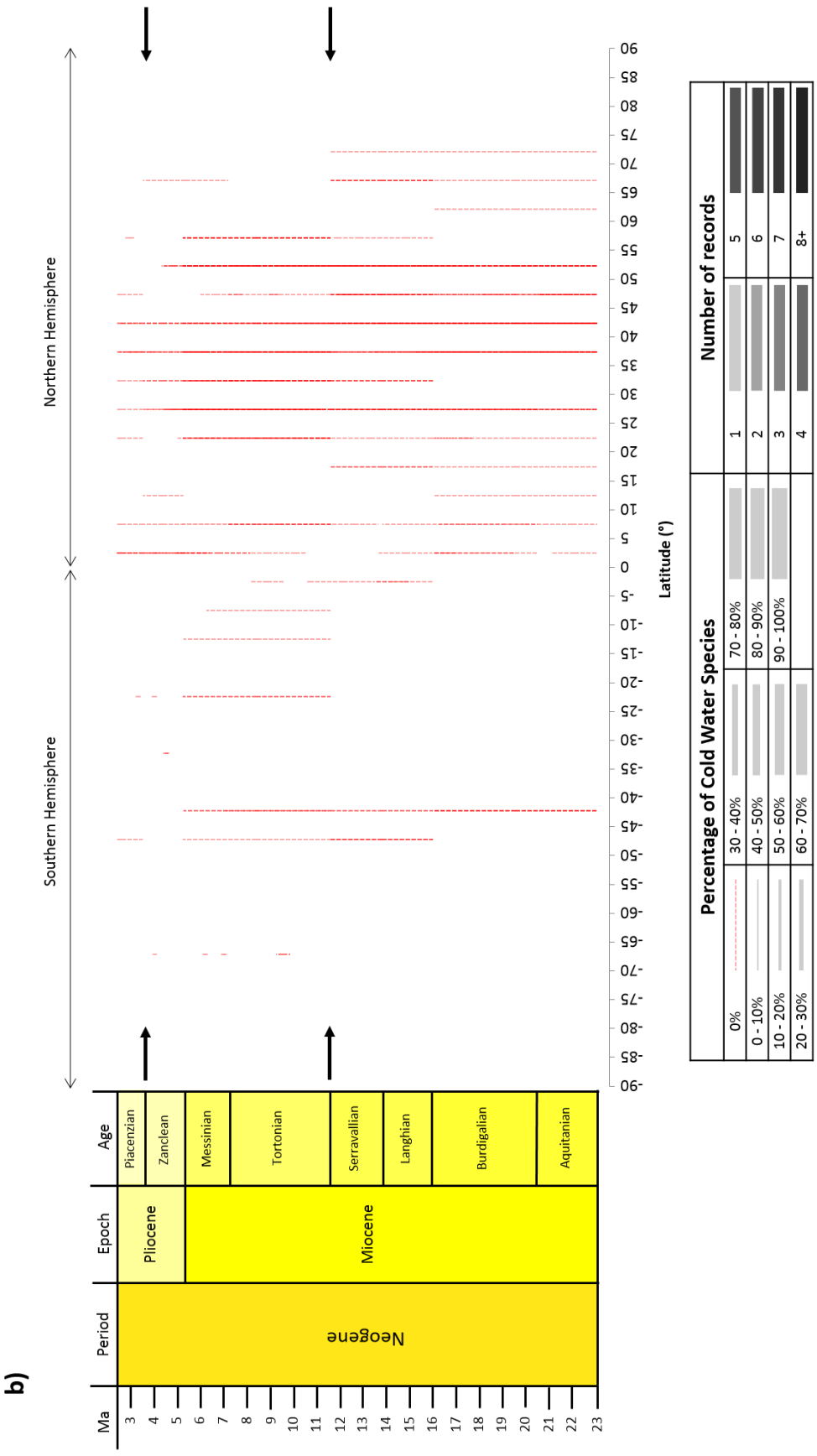

Figure 5: Dinoflagellate cyst data for the entire Neogene is divided into latitudinal bins spanning five degrees. There are consistently more data for the Northern Hemisphere than the Southern Hemisphere. For each record, the percentage of

CWS was calculated relative to the number of species with known temperature preferences. The percentage of CWS is displayed and is represented by the horizontal thickness of the line. The shading of the lines represents the number of records present within each latitudinal bin. Dashed red lines represent records with no CWS. Figure 5a represents all records and Figure 5b contains only those records with no CWS present. Arrows indicate the two main periods of cooling. To help explore uncertainties, the number of records found within each latitudinal bin is represented by the shading. The darker the shading, the more data are present, and therefore the more reliable the signal is likely to be.

4.4 Pliocene (5.333–2.58 Ma)

In the Zanclean and Piacenzian (Figure 4g, h), the mean percentages of CWS between 0 and 45° N are all under 7%. The exception are data from between the latitudes of 10 to 15° N, which has a mean CWS percentage of 17%. The mean percentages of CWS north of 55° N are all over 20%, and above 75° N they are 87% or higher. Globally, the mean percentages of the Zanclean and Piacenzian are 17 and 28%, which are very similar to the values calculated when using data exclusively from the Northern Hemisphere (17 and 27%). The proportion of records with CWS present attained as high as 71% in the Piacenzian and the proportion of CWS making up each record increases particularly between the Zanclean and the Piacenzian. For example, in the Piacenzian records, CWS percentages of 11 to 15% appear in the Mediterranean. Records where all of the species with known temperatures preferences are CWS can be found north of Canada, east of Greenland and west of Svalbard.

4.5 Modern surface sediments

Data for surface sediments comes from Zonneveld et al. (2013b). There is a significantly higher number of sites in the modern than for the Neogene and a broad global distribution is achieved (Figure 4i). However, as in the Neogene, there are fewer records for the Southern Hemisphere compared to the Northern Hemisphere, and the Indian and Pacific oceans are also under-represented (Figure 4i). For the majority of ocean basins, most of the records come from the coasts, and relatively few come from deeper and more oceanic regions. Sites that are composed only of CWS are common in higher latitudes in both the Southern and Northern Hemispheres. In the lower

latitudes, species with known temperatures are nearly all WWS. Between 20° N and 20° S, there are only four records (out of 377) that contain any CWS. Three of these are found off the west coast of Africa and the fourth is off the east coast of Africa, all have CWS percentages under 10%. Records composed entirely of CWS are common above and below 45° N and 45° S, respectively. Asymmetry occurs either side of the North Atlantic. Records where all of the species with known temperature preferences are CWS reach as far south as 42° N on the western edge of the North Atlantic, but only as far south as 56° N on the eastern side. This likely stems from the presence of the North Atlantic Current, which transports warm water to the higher latitudes of the northeast North Atlantic Ocean.

The global mean percentage of CWS for surface sediments is substantially higher than for the stages of the Neogene (38%; Figure 6a), as is the mean percentage when comparing just the Northern Hemisphere (43%; Figure 6b). When calculating the mean percentage of CWS for just those latitudes where data is present for the Neogene, the mean percentage of CWS is still high at 34% (Figure 6b). In the modern (Figure 5i), between 0 and 35° N, the mean percentages of CWS relative to WWS are all under five percent, which quickly rises to 50% and above north of 45° N (Figure 7i).

An example of where the spread of data influences the results can be seen in the modern map (Figure 4i). There are a very high number of records (95) in the Gulf of St. Lawrence, on the east coast of Canada, contributing 33% of all the records between 45 and 55° N. In 72 of these records, all the species with known temperature preferences are CWS (mostly *Spiniferites elongatus* and *Islandinium minutum*). The remaining 13 records from the Gulf of St. Lawrence have CWS percentages between 50 and 83%. These results indicate that the Gulf of St. Lawrence is particularly cold compared to the rest of the oceans at this latitude (Figure 7i). It is a small, restricted basin that receives a large quantity of freshwater and has limited exchange with the open ocean (Long et al., 2015). The only open ocean water source is through the Belle Isle Strait, bringing cool Labrador Sea water into the Gulf. However, the majority of the cool waters form *in situ* during the winter season (Banks, 1966; Saucier et al., 2003). The plethora of sites reflecting the cool water Gulf of St.

Lawrence microclimate produces a noticeable feature in the modern. In the modern 45–55° N latitudinal bins, the mean percentage of CWS relative to WWS is significantly higher than it was in the 40–45° N latitudinal bin (Figure 7i). If the 95 records from the Gulf of St. Lawrence are removed from the analysis, this step like change seen at roughly 45° N is no longer present, providing a clear example of how a large number of records in a small region can alter the global signal, and demonstrating why it is preferable to have an even spatial coverage of data.

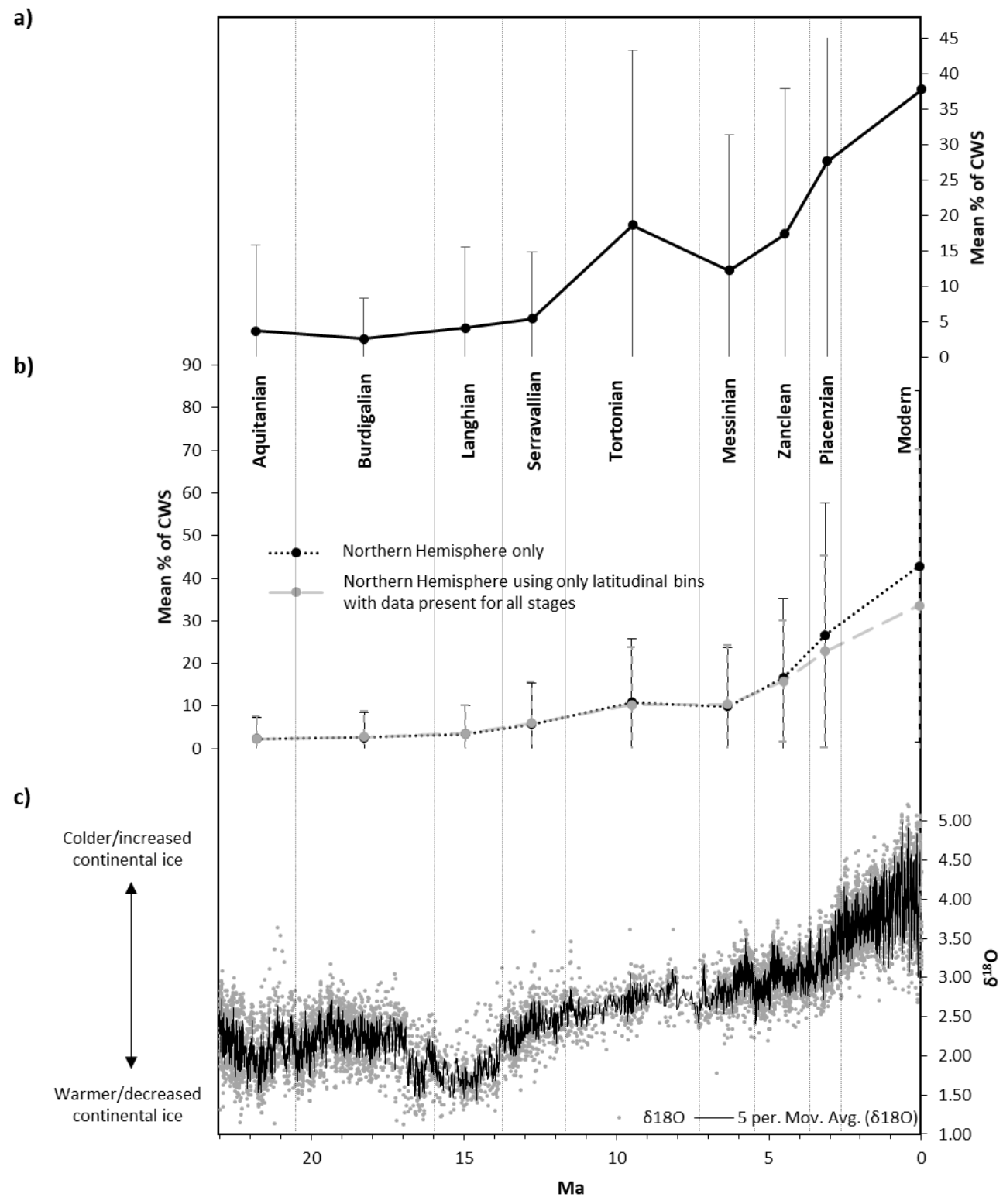

419

420

421 **Figure 6: Mean percentages of Cold Water Species (CWS) of dinoflagellate cysts for each stage for (a) all records, (b) only**

422 **records from the Northern Hemisphere and using only the latitudinal bins (in the Northern Hemisphere) where data are**

available for all stages. (c) Benthic $\delta^{18}O$ compilation (Zachos et al., 2001; 2008) demonstrating cooling through the Neogene to present for comparison with the mean percentage of CWS. Error bars are included in panels a and b and represent the standard deviation. In general the error bars are larger in the younger time intervals. This is due to the increasing latitudinal temperature gradient and, as a result of this, the percentage of CWS in each assemblage becomes more variable through time.

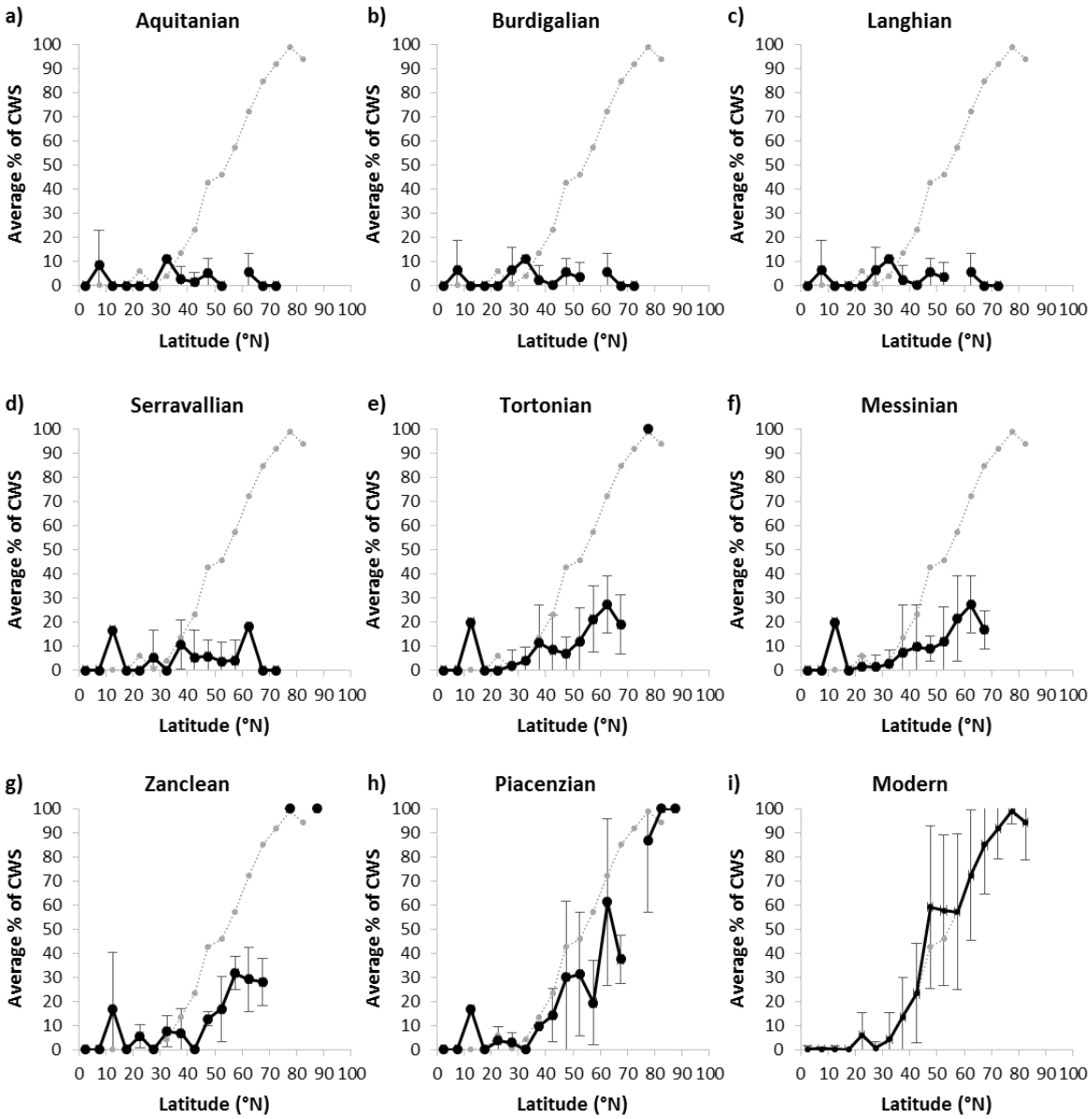

Figure 7: The mean percentage of Cold Water Species (CWS) of dinoflagellate cysts relative to the total number of species present with known temperature preferences for each five degree latitudinal bin. (a) Aquitanian, (b) Burdigalian, (c) Langhian, (d) Serravallian, (e) Tortonian, (f) Messinian, (g) Zanclean, (h) Piacenzian and (i) the modern. For the modern, results were replotted without data from the Gulf of St. Lawrence (grey dotted), a densely sampled region, to

investigate sampling bias. This grey dotted line is included in all stages for comparison. Error bars represent the standard deviation.

4.6 The pull of the recent and the latitudinal biodiversity gradient

Temperature preferences of dinoflagellate cysts are better known for those species that are either extant or most recently became extinct. This phenomenon is known as 'the pull of the recent' and was originally conceived for diversity studies, particularly in the Cenozoic (Raup, 1979; Jablonski et al., 2003). If the pull of the recent was affecting the results, it is possible that the increasing number of CWS in successively younger stages is due to a better understanding of the temperature preferences of dinoflagellate cysts. It is for this reason that the main analysis compared the proportion of CWS to WWS, rather than the absolute number of CWS present (Figures 3, 4). However, with the exception of the Early Miocene, which has the fewest species with known temperature preferences (Figure 8; five CWS and 30 WWS), the pull of the recent does not seem to have influenced the rest of the Neogene, and the number of species found in each stage is highest for the Tortonian (Figure 8). It is also worth noting that when the percentage of CWS and WWS (present in each stage) is calculated relative to each other (Figure 8), the percentage of CWS in each stage increases through the Neogene with the cooling temperatures. As the pull of the recent presumably affects CWS and WWS equally, suggesting the CWS and WWS ratio is unaffected (Figure 8; black dashed line), we surmise that the increase in the proportion of CWS relative to WWS through the Neogene is a robust feature of the dataset caused by the cooling climate.

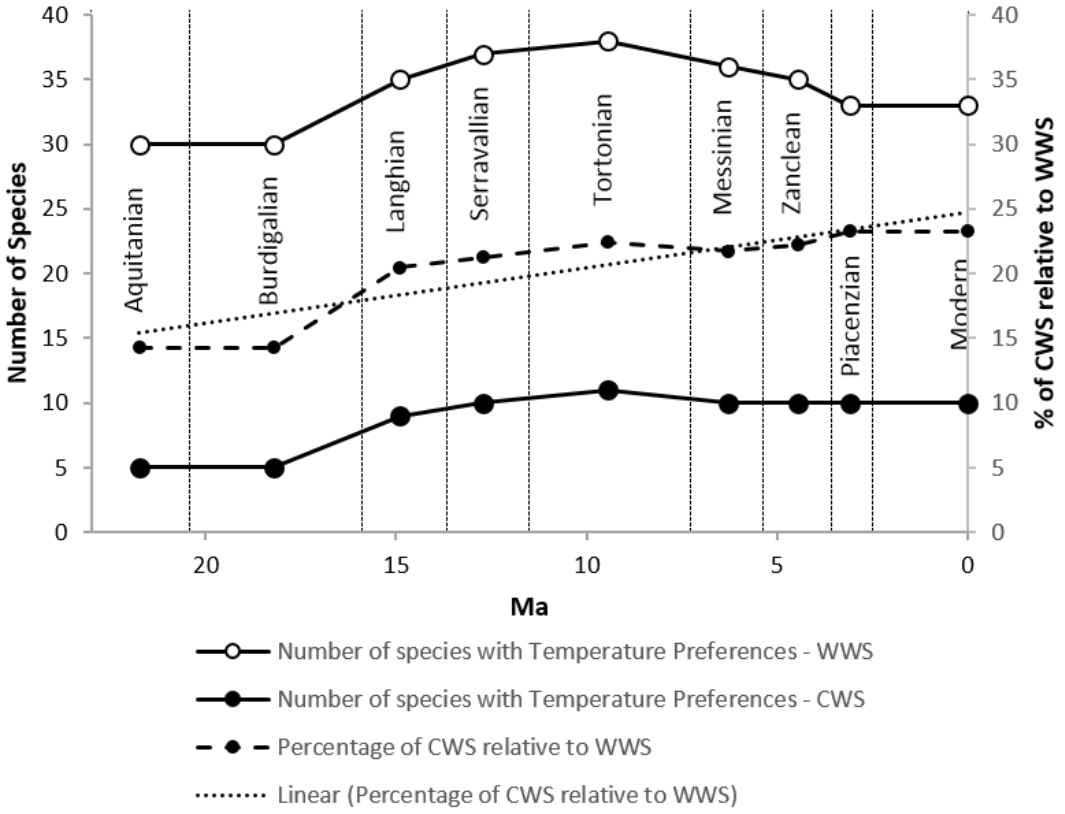

452

453 **Figure 8: The number of dinoflagellate cyst species with warm or cold water preferences for each stage are plotted on**
454 **the left axis and the percentage of Cold Water Species (CWS) that make up the total number of species with known**
455 **temperature preferences for each stage (black dashed line) are plotted on the right axis. The data were obtained by**
456 **counting the number of species in each stage from the range chart in Figure 3.**

457 Throughout the Neogene, there is a significantly higher number of WWS than CWS (Figure 8). This is
458 likely due to the latitudinal biodiversity gradient where the warmer, lower latitudes have a higher
459 diversity than the cooler, higher latitudes. This phenomenon has been observed in the geological
460 record for at least the last 30 Myr (Crame, 2001; Mittelbach et al., 2007; Mannion et al., 2014). This
461 relatively low species richness of CWS is an enduring feature of the dinoflagellate cyst record, and
462 hence does not affect our interpretations. There are fewer localities in the most northerly/southerly
463 latitudes, which potentially led to higher numbers of WWS compared to CWS in the database.
464 However, as this is consistent throughout the Neogene, it is unlikely to bias our results.

465

4.7 Uncertainty from geographical and temporal distribution of data

The majority of CWS occurrences are in the Northern Hemisphere (Figure 4). This is a clear sampling bias due to the lack of Neogene dinoflagellate cyst records from the Southern Hemisphere (Figure 4). For this reason, the mean percentage of CWS for each stage (Figure 6a) was recalculated only using the records from the Northern Hemisphere (Figure 6b). The most obvious difference between the two methods (global versus northern only) was in the Tortonian. The mean percentage of CWS was higher for the Tortonian than for the immediately adjacent stages. This difference for the Tortonian can be explained by the Southern Hemisphere having substantially more records than in the other time intervals (Figures 4e, 5a), the majority of which have CWS values of 33% or higher. These records, between 65 and 70° S and 20 to 25° S, are numerous, with tightly constrained ages, and result in a much larger percentage of CWS in the Tortonian (19%, Figure 6a) than in the stages below and above (5% in the Serravallian and 12% in the Messinian). When only using data from the Northern Hemisphere, which has a more equal spatial distribution, there is a reduced discrepancy between the Tortonian and the immediately adjacent stages (Figure 6b). It is for this reason that the conclusions drawn from this study mainly concern the Northern Hemisphere. As the majority of data in the Northern Hemisphere were collected from the North Atlantic and Arctic oceans and the Mediterranean region, it is likely that the signal produced is from those areas, rather than for the whole of the Northern Hemisphere.

This implies that care must also be taken in the Northern Hemisphere in latitudinal bins that are devoid of data for some of the stages. For example, the three most northerly latitudinal bins only have data for the Pliocene, all of which have high percentages of CWS. To ensure that the Pliocene data were not skewing the results, further analysis of the data was carried out excluding latitudinal bins that did not have data for all stages (Figure 6b). Comparing results using all the Northern Hemisphere data, to those using simply latitudinal bins with data present for every stage (Figure 6b), indicates that the cooling was more extreme when all the data for the Northern Hemisphere were

used. However, the overall trend is the same, and leads to the conclusion that the absence of data in the high latitudes for stages other than the Pliocene has not skewed the results.

The average age range of the records for each stage is variable (Figure 9). The records from the Aquitanian and Burdigalian have the longest age range (4.7 and 4.4 Myr respectively), and the Zanclean and Piacenzian records have the shortest age ranges (0.9 and 0.8 Myr respectively). This is partly due to the nature of the dating. For example, many of the records dated in the literature are dated to within a stage or in some cases, to the nearest sub-epoch (i.e. the Early Miocene). Thus, the records of the longer stages, such as the Burdigalian (spanning 4.47 Myr) have a higher average age range, while the Piacenzian (the shortest stage of the Neogene; 1.02 Myr in duration) has a much lower average record length. Unfortunately, this means that any evidence of short scale events affecting dinoflagellate cysts, such as the MMCO and the mPWP, is not resolved in this study. Further to this an individual data-set may fall into either a “warm” or “cold” phase of the Neogene orbital cycle (Salzmann et al., 2013; Liebrand et al., 2017). If all the records used to define the %CWS for a stage were to come from a “warm” phase, then a “cold” phase result might be biased in that direction. Despite this uncertainty in the time-averaging approach applied to Neogene dinoflagellate cyst records a trend from low %CWS during the Early Miocene to high %CWS in the Late Pliocene is seen. It is therefore still possible to interpret long-term changes and, in the future, the generation of higher-resolution dinoflagellate cyst records would facilitate more detailed studies of climate and environmental change.

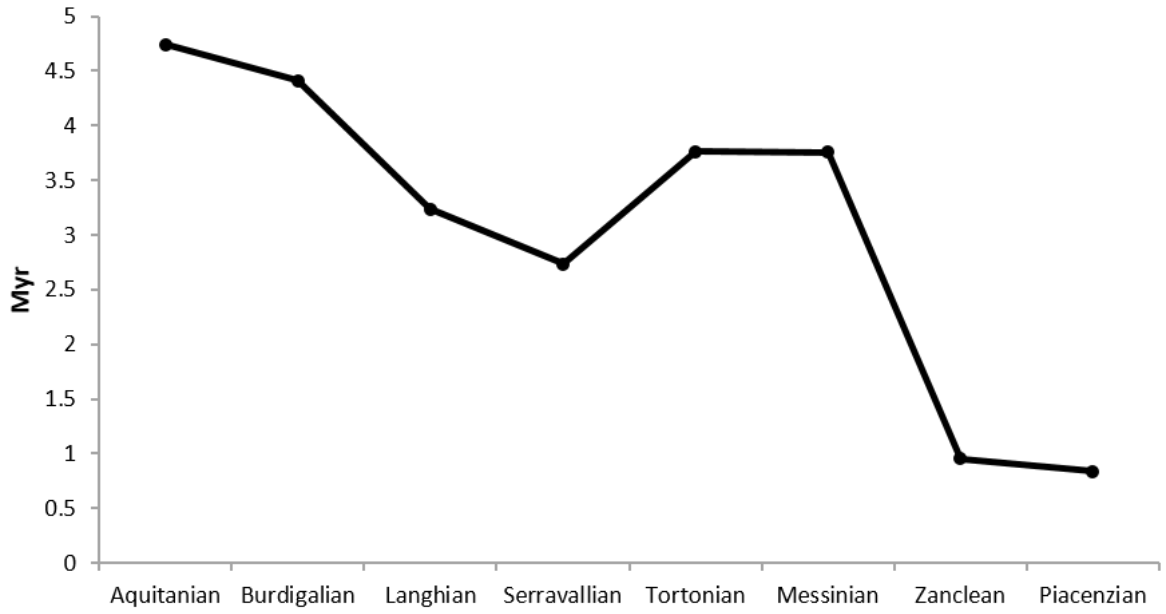

Figure 9: The average duration of dinoflagellate cyst records for each stage. Generally, temporal resolution of the data is higher in shorter stages because much of the data are dated to within a stage.

5. Discussion

5.1 Driving factor of the cooling Neogene

The increase in CWS through the Neogene (Figures 6, 7) strongly supports the cooling trend seen in the benthic oxygen isotope stack, global vegetation records and global alkenone data (Zachos et al., 2008; Pound et al., 2012a; Salzmann et al., 2013; Utescher et al., 2015; Herbert et al., 2016). Dinoflagellate cyst species that indicate cold waters are largely absent from the Aquitanian to the Serravallian (Figures 6, 7). This was followed, in the Late Miocene and Pliocene, by increasing proportions of CWS at individual data sites and the biogeographical expansion of cold water dinoflagellate cysts species towards the lower latitudes (Figures 4, 7). By the Piacenzian, a forerunner of the modern latitudinal distribution of CWS was present (Figure 7). The global scale changes in dinoflagellate cysts through the Neogene points to a global scale control on Neogene climate. The most likely candidate would be changing concentrations of atmospheric CO_2 (Pound et

al., 2011; 2012a; Bolton and Stoll, 2013). The role of CO_2 in driving Pliocene climate is well established (Haywood et al., 2016), whilst it has been strongly debated whether Miocene climate was also controlled by atmospheric CO_2 (Knorr et al., 2011; Pound et al., 2011; Bradshaw et al., 2012; Forrest et al., 2015). Much of the argument stems from older records of marine proxies for CO_2, which show flat-lining atmospheric CO_2 or values below the pre-industrial standard of 280 ppmv for most of the Miocene (Pagani et al., 1999; 2005; Beerling and Royer, 2011). The counterarguments to these lines of evidence have been that these CO_2 records are incorrectly calculated (Ruddiman, 2010) and/or the true Miocene CO_2 level has yet to be detected in the record (Bolton and Stoll, 2013).

More recent records of Neogene CO_2 have demonstrated higher atmospheric values and high-resolution fluctuations that are in tune with other climate proxy records (Zhang et al., 2013; Greenop et al., 2014). Carbon dioxide as a controlling factor on Neogene climate is consistent with the global scale changes in CWS dinoflagellate cysts (Figures 4, 7). Modelling results compared to global datasets consistently show that higher (ca. 360-500 ppmv) CO_2 levels are necessary for successful simulation of Neogene climates (Dowsett et al., 2013; Bradshaw et al., 2015; Haywood et al., 2016; Stap et al., 2016). The global increases in Neogene cold water dinoflagellate cysts species are in agreement with the benthic $\delta^{18}O$ isotope stack (Zachos et al., 2008), global changes in biome distribution through the Neogene (Pound et al., 2012a; Salzmann et al., 2013), reconstructed marine and terrestrial temperatures (Utescher et al., 2015; Herbert et al., 2016), and the isotopic divergence of coccolithophores (Bolton et al., 2012; Bolton and Stoll, 2013). Such diverse and widespread evidence for a large-scale driver of global climate points to an overarching role of atmospheric CO_2.

5.2 The Early Miocene (23.03–15.97 Ma)

Immediately prior to the Miocene, the Mi-1 event (23.13 Ma, Abels et al., 2005) in the benthic oxygen isotope record shows a shift to cooler bottom waters and/or increased ice accumulation on Antarctica (Zachos et al., 2001; Billups and Schrag, 2002; Wilson et al., 2013; Beddow et al., 2016;

553 Liebrand et al., 2017). Recent high-resolution research has clearly demonstrated that there is much
554 more detail in the benthic oxygen isotope records than can be described using the traditional
555 Mi oxygen isotope glaciations/zones (Miller et al., 1991; Liebrand et al., 2017; Paul A. Wilson,
556 personal communication 2017). However this contribution is a global review, and we retain the Mi
557 terminology because the aim here is to compare intercontinental changes in CWS dinoflagellate
558 cysts with broad-scale perturbations in Neogene palaeoclimates. We do not propose correlations to
559 specific oxygen isotope stratigraphies.

560 Whilst evidence for ice sheets in the Northern Hemisphere is uncertain, sea-ice was present in the
561 Arctic (Larsen et al., 1994; Moran et al., 2006, DeConto et al., 2008). Ice accumulation at one or
562 potentialy both poles indicates a relatively cool climate, however, the mean CWS percentage of 2%
563 for the Aquitanian and 3% for the Burdigalian is more indicative of globally warmer oceans (Figure
564 4a, b). With the exception of occurrences off the Antarctic Peninsula, the CWS of the Aquitanian and
565 Burdigalian are not at the high latitudes and can be compared to the occurrence of CWS in the
566 modern Mediterranean Sea (Zonneveld et al., 2013b). The low numbers of CWS during the Early
567 Miocene indicates that the latitudinal temperature gradient was considerably flatter than at present
568 (Figure 7a, b). This was previously suggested by Nikolaev et al. (1998) from a compilation of
569 foraminifera and oxygen isotope data. The Early Miocene was not an interval of sustained warmth;
570 alkenone data from the Paratethys Sea shows a 2–3 °C cooling between 18.4 and 17.8 Ma (Grunert
571 et al., 2014). The Early Miocene is characterised by a 2.4 Ma eccentricity-paced benthic oxygen
572 isotope record with distinct intervals of glacial-interglacial cycles operated on a 110 ky periodicity
573 (Liebrand et al., 2017). These rapid climate and cryosphere changes are not detected in the present
574 study due to low dating resolution in many dinoflagellate cyst studies (Figure 9).

575 ## 5.3 The Mid Miocene (15.97–11.62 Ma)

576 The Mid Miocene is both an interval of sustained global warmth (MMCO; 17-14.5 Ma) and one of
577 step-like global cooling at Mi-3a, Mi-3b, Mi-4 and Mi-5 (ca. 14-11.6 Ma; Savin et al., 1975; Shackleton

578 and Kennett, 1975; Zachos et al., 2001; Böhme, 2003; You et al., 2009; Quaijtaal et al., 2014). This
579 general pattern of a warm Langhian and a cooling Serravallian is recorded in the percentage of CWS
580 in each stage but higher-resolution changes in temperature are not visible due to the time slab
581 approach of the current study (Figure 6a, b). Towards the end of the Early Miocene, benthic $\delta^{18}O$
582 values rapidly decreased, suggesting a reduction in continental ice and a global warming event
583 (Zachos et al., 2001; 2008). The warming event culminated in the MMCO and resulted in the tropical
584 climate zone having a much greater latitudinal extent, abundant precipitation and decreased
585 seasonality (Böhme, 2003; Bojar et al., 2004; Kroh, 2007; Pound et al., 2012a). Even though mean
586 global temperatures in the MMCO were more than 3°C higher than today (Pagani et al., 1999;
587 Kürschner et al., 2008; You et al., 2009; Foster et al., 2012), evidence for this relatively short
588 duration of warming is not obvious in this study, likely due to a lack of temporally high-resolution
589 data in the TOPIS database.

590 In addition to increased temporal resolution, improved reporting of abundance data would help to
591 identify events such as the MMCO using TOPIS. For example, Warny et al. (2009) detected the
592 MMCO in Antarctica by a 2000-fold abundance increase of just two species. These authors
593 associated the peak in productivity with increased meltwater runoff from the elevated temperatures
594 of the MMCO (Warny et al., 2009). This demonstrates how routine reporting of abundance data in
595 the literature would enhance our ability to understand Neogene climate trends.

596 What is evident from the database, is that a cooling trend occurred between the Langhian and the
597 Serravallian, which resulted in a slight increase in the percentage of CWS (Figure 6a, b). Whilst this
598 small change is apparent, it is not as characteristic as the step-like cooling demonstrated by benthic
599 $\delta^{18}O$ values during the Serravallian (Figure 6c; Quaijtaal et al., 2014). Instead, the Serravallian
600 consistently has higher percentages of CWS than preceding stages, indicating that dinoflagellate
601 cysts did respond to the cooling, but not uniformly in the surface waters at all latitudes. This may
602 relate to the asymmetrical nature of the cooling; the latitudinal temperature gradient steepened

603 first in the Southern Hemisphere during the Serravallian in response to the expansion of Antarctic ice
604 sheets (Pound et al., 2012a). Whilst the Northern Hemisphere (in the North Atlantic region at least)
605 maintained a shallower gradient, possibly in response to the onset of the warm Gulf Stream ocean
606 current (Denk et al., 2013).

607 Although the benthic $\delta^{18}O$ values significantly increased in the Serravallian, and less in the Tortonian,
608 the dinoflagellate cyst record (Figure 6a-c) demonstrates the opposite. Thus, a more significant
609 cooling is indicated in the Tortonian as opposed to the Serravallian. This suggests either a time-
610 averaged response of dinoflagellate cysts to the step-like cooling of the Serravallian, or that the
611 surface waters cooled at a different rate to the deep waters. Global biome reconstructions also
612 demonstrate that the cooling was more pronounced between the Serravallian and the Tortonian,
613 than the Langhian and the Serravallian (Pound et al., 2012a). This may reflect a growth of ice sheets
614 during the Serravallian, whereby the increase in deep water $\delta^{18}O$ values records a combination of
615 cooling and ice accumulation (Badger et al., 2013; Knorr and Lohmann, 2014), whereas the Late
616 Miocene did not have any additional permanent ice, but underwent continued global cooling
617 (Herbert et al., 2016). In addition, vegetation records (Pound et al., 2012a) demonstrate that the
618 Southern Hemisphere cooled prior to the Northern Hemisphere, and as the majority of the records
619 used in this study are from the Northern Hemisphere, this could be a further explanation for the
620 delayed response of the dinoflagellate cysts to the signal produced by the benthic $\delta^{18}O$ values
621 (Zachos et al., 2001; 2008).

622 During the Langhian the Central American Seaway (CAS) shoaled, potentially preventing deep water
623 exchange from around 15 Ma (Montes et al., 2015). Unfortunately there are currently no
624 dinoflagellate cyst records in TOPIS for the Caribbean during the Mid Miocene (Figure 4). However,
625 this shoaling or closure would have modified ocean circulation, and modelling results have shown
626 that this warms the Northern Hemisphere (Brierley and Federov, 2016; Lunt et al., 2008). This is
627 consistent with the low numbers of CWS dinoflagellate cysts in the high latitudes of the Northern

628 Hemisphere (Figure 4). The closure of the CAS during the Langhian would have promoted heat
629 transport into the North Atlantic. It would also have tempered the global cooling of the post-MMCO
630 climate as seen in Northern Hemisphere floras (Denk et al., 2013) and strengthened the
631 asymmetrical latitudinal temperature gradient (Pound et al., 2012a).

632 ## 5.4 The Late Miocene (11.62–5.33 Ma)

633 The Late Miocene, though still significantly warmer than the present, was considerably cooler than
634 the Mid Miocene (Pound et al., 2012a; Utescher et al., 2015) and the Tortonian in particular (11.62–
635 7.25 Ma) was characterised by warmer and more humid conditions than today (Bruch et al., 2006;
636 Pound et al., 2011). This is reflected in the increased percentage of, and wider biogeographical
637 distribution of, CWS dinoflagellate cysts (Figures 4, 5). Mean annual temperatures were between 14
638 and 16 °C in northwest Europe (Donders et al., 2009; Pound et al., 2012b; Pound and Riding, 2016).
639 Furthermore, the Cenozoic global cooling trend, which resumed at the end of the MMCO, continued
640 (Zachos et al., 2001). However, benthic $\delta^{18}O$ values demonstrated that the cooling was more gradual
641 for the Tortonian compared to the Serravallian, assuming that there was no additional ice sheet
642 growth (Figure 6c; Zachos et al., 2008). This cooling affected the presence of cold water
643 dinoflagellate cysts, and the mean percentage of CWS reached 10% in the Tortonian (Figure 6b).

644 The dinoflagellate cyst record is consistent with global vegetation records that show a cooler, more
645 seasonal, biome distribution in the Northern Hemisphere in the Tortonian, than during the
646 Serravallian (Pound et al., 2012a). Furthermore, pollen-based temperature reconstructions from
647 New Zealand demonstrate Southern Hemisphere cooling immediately after the MMCO (Prebble et
648 al., 2017). The percentage of CWS in the Tortonian in the mid to high latitudes increased, while the
649 percentage in the low latitudes remained similar to the values for the Early and Mid Miocene
650 (Figures 7a-e). The Tortonian was also the earliest stage to have all dinoflagellate cysts with known
651 temperature tolerances being CWS at 75–80° N. This indicates substantial high latitude cooling by
652 this time during the Neogene, which is consistent with proxies for extensive seasonal sea ice in the

Arctic during the Tortonian (Stein et al., 2016). The increase in the percentage of CWS in the higher latitudes compared with the low latitudes reflects that tropical regions during the Miocene remained at similar temperatures, whereas the high latitudes cooled (Nikolaev et al., 1998; Williams et al., 2005; Steppuhn et al., 2006; Herbert et al., 2016). This effect caused the latitudinal temperature gradient to steepen throughout the Late Miocene and Pliocene in the Northern Hemisphere (Nikolaev et al., 1998; Crowley, 2000; Fauquette et al., 2007; Pound et al., 2012a). This temperature decrease in the high latitudes was described by Nikolaev et al. (1998), who demonstrated a 4–6 °C increase in the latitudinal temperature gradient between 10 and 5 Ma. Cooling of the mid to high latitude surface waters during the Late Miocene is also reflected in the alkenone sea surface temperature reconstructions (Herbert et al., 2016)

Global temperatures continued to cool through the Messinian (Pound et al., 2012a; Utescher et al., 2015; Herbert et al., 2016; Stein et al., 2016). However, the benthic oxygen isotope record does not show a clear signal towards colder bottom water temperatures in conjunction with the evidence for surface cooling (Zachos et al., 2008). Widespread alkenone data suggest that the Messinian included some of the largest cooling in sea surface temperatures of the Late Miocene, and a temperature minimum is recorded in the Arctic at around 6.5 Ma (Herbert et al., 2016; Stein et al., 2016). Despite this, the geographical distribution and percentages of CWS dinoflagellate cysts are similar to the Tortonian (Figures 4, 7). This may be an artefact of the time-slab approach, or the current available data on global dinoflagellate cysts. Much of the information on Messinian dinoflagellate cysts comes from the North Atlantic, which by the Late Miocene was under the influence of the Gulf Stream current (Denk et al., 2013). Many of the records also lack the necessary age control and resolution to identify short-lived cooling events witnessed in other records (Herbert et al., 2016; Stein et al., 2016). The globally distributed alkenone based sea surface temperature reconstructions suggest near modern temperatures between 7 and 5.4 Ma (Herbert et al., 2016). This time interval is also one of a stable climate state, with potentially higher ice volumes and a greater threshold for deglaciation (Drury et al., 2016). However, near modern temperatures during the Messinian are not

consistent with Arctic surface water temperatures, dinoflagellate cysts, faunal distributions or global vegetation records (Donders et al., 2009; Pound et al., 2012a; Utescher et al., 2015; Azpelicueta and Cione, 2016; Stein et al., 2016; Prebble et al., 2017).

The presence of CWS dinoflagellate cysts in the Late Miocene of offshore South Africa (Figure 4) has been used as an indicator for the presence of the cold Benguela Current (Siesser, 1980; Diester-Haass et al., 1990; Robert et al., 2005; Heinrich et al., 2011; Hoetzel et al., 2017). The slightly reduced number of cold water dinoflagellate cysts in the Mediterranean during the Messinian, when compared to the Tortonian, is in agreement with alkenone data that shows warmer Messinian Sea Surface Temperatures (SSTs) than in the latest Tortonian (Tzarnova et al., 2015). The temporal resolution of the dataset does not allow any response to the Messinian Salinity Crisis to be detected (Flecker et al., 2015), especially since the global-scale climate effects would have been limited in magnitude and extent, and transient (Ivanovic et al., 2014).

5.5 The Pliocene (5.33–2.58 Ma)

In the Pliocene, the trends towards cooler climates continued and was interrupted by brief warm intervals (Haywood et al., 2013; 2016; Salzmann et al., 2013). Despite being cooler than the Miocene, the Pliocene was still significantly warmer than today (Haywood et al., 2013; Salzmann et al., 2013; Pound et al., 2015; Dowsett et al., 2016; Panitz et al., 2016) with a shallower Northern Hemisphere latitudinal gradient of CWS-dominated dinoflagellate cyst assemblages compared to the modern (Figure 7). The percentage of CWS increased most markedly in the high latitudes, from 45° N northwards (Figure 7e, f), thereby further steepening the latitudinal temperature gradient. Nikolaev et al. (1998) found that the latitudinal gradient increased by 4–5 °C during the Piacenzian, and Fedorov et al. (2013) demonstrated a 4–7 °C cooling of the mid to high latitudes of the North Atlantic and Pacific oceans. This cooling of the higher latitudes compared to the lower latitudes is a characteristic observed using a variety of proxies (Nikolaev et al., 1998; Brierley and Fedorov, 2010;

703 Pound et al., 2012a; Federov et al., 2013; Herbert et al., 2016), and was associated with the
704 development of ice in the high latitudes (Dolan et al., 2011; Dowsett et al., 2016).

705 Short-lived glaciations were infrequent in the Zanclean, but became more common in the Piacenzian
706 as the global climate continued to cool (Lisiecki and Raymo, 2005; Miller et al., 2005; 2012). A
707 generally warmer Zanclean, and a cooler Piacenzian, is consistent with the average percentage of
708 CWS dinoflagellate cysts in the Zanclean (16%) and the Piacenzian (23%; Figure 4), and is consistent
709 with global alkenone records (Herbert et al., 2016). However, short-lived glaciations are not
710 currently detectable in the TOPIS database due to the limitations of sampling resolution. The East
711 and West Antarctic ice sheets were both well established by this time (Naish and Wilson, 2009;
712 Dolan et al., 2011). Although the Southern Hemisphere lacks widespread dinoflagellate cyst records
713 for the Piacenzian, the two data points proximal to the Antarctic Peninsula contain 100% CWS
714 dinoflagellate cysts (Figure 4). Ice sheets in the Northern Hemisphere were significantly smaller,
715 compared to the modern, or absent, which is consistent with WWS dinoflagellate cysts still being
716 present in the high latitudes of the North Atlantic (Figure 4; Dolan et al., 2011; De Schepper et al.,
717 2014; Panitz et al., 2016). Global climate started to significantly deteriorate (cooled) in the
718 Piacenzian, leading to the intensification of the Northern Hemisphere glaciation around 2.75 Ma
719 (Ravelo et al., 2004; Mudelsee and Raymo, 2005; De Schepper et al., 2014; Panitz et al., 2016).

720 The CAS continued to constrict during the Pliocene before finally closing around the Pliocene–
721 Pleistocene boundary (Coates and Stallard, 2013; Osbourne et al., 2014). Neodymium isotopes show
722 the exchange of waters until 2.5 Ma, but deep water exchanges had ceased by 7 Ma (Coates and
723 Stallard, 2013; Osbourne et al., 2014). Interhemispheric foraminifera based Mg/Ca and $\delta^{18}O$ suggest
724 that this continued constriction lead to greater heat transport in the Zanclean into the Northern
725 Hemisphere, but reduced heat transport during the Piacenzian (Bailey et al., 2013; Karas et al.,
726 2017). These results are consistent with the latitudinal distribution of CWS dinoflagellate cysts in the
727 Zanclean and Piacenzian (Figures 4, 7).

6. Conclusions

Global datasets compiling previously published data are becoming more common and are increasingly used for evaluating environmental and climatic changes over longer time scales and over large regions (Salzmann et al., 2008; Masure and Vrielynck, 2009; Pound et al., 2012a; Masure et al., 2013; Woods et al., 2014). In our global compilation of Neogene dinoflagellate cyst data, we observed an increase in the mean percentage of CWS from the Early Miocene to Late Pliocene. An increase in the percentage of CWS, relative to the total number of species present with known temperature preferences, is qualitative evidence for decreasing SSTs. Our results agree very well with the gradual global climate cooling over the Neogene and increasing continental ice volume (Figure 6c; Zachos et al., 2001; 2008; Billups and Schrag, 2002; Ravelo et al., 2004; Shevenell et al., 2004; McKay et al., 2012; Miao et al., 2012; Pound et al., 2012a; Lear et al., 2015, Herbert et al., 2016). Our global compilation also allowed distinction between large scale climatic changes and local anomalies; for example, determining if the cooling trend had a global latitudinal and/or longitudinal gradient in the Miocene, Pliocene and modern surface ocean. From this study, the following conclusions can be drawn in relation to the research questions outlined in the introduction:

Can dinoflagellate cysts be used to determine global cooling in the Neogene?

- Dinoflagellate cysts are increasingly being used in palaeoclimate studies and this work corroborates their usefulness as a qualitative and relative temperature indicator over long timescales. Dinoflagellate cysts with known temperature preferences can be used to determine cooling on a global scale and the general cooling trend shown in this study broadly agrees with the global climate evolution in the Neogene (Figure 6c; Zachos et al., 2008). Our approach is validated by successful reconstructions of the modern sea surface temperature distribution on a global scale (Figure 4i, j).

Was the cooling during the Neogene uniform at all latitudes?

- Increases in the CWS percentage occurred most prominently in the mid to high latitudes, and less in the lower latitudes throughout the Neogene. This suggests that the mid to high latitudes underwent more cooling than the lower latitudes, at least in the Northern Hemisphere (Figure 7). The lower latitudinal temperature gradient during the Early and Mid Miocene, implied by smaller percentages of CWS in all latitudinal bins, agrees with terrestrial reconstructions from Pound et al. (2012a). These authors described a steepening of the latitudinal temperature gradient, as the high latitudes cooled more than the lower latitudes.

Was the rate of cooling uniform across the whole Neogene?

- Neogene climate cooling did not always occur at a steady rate and the most significant cooling occurred in the Pliocene, between the Zanclean and the Piacenzian (Figure 6a, b). There was a further decrease in temperature between the Piacenzian and the modern (Zonneveld et al., 2013b). The faster cooling rate from the Pliocene to the modern is consistent with the benthic $\delta^{18}O$ curve of Zachos et al. (2008).

Further progress in the global application of dinoflagellate cysts would be made with the collection of more primary data. In particular, targeting the Indian and Pacific oceans and the Southern Hemisphere throughout the entire Neogene would substantially improve our knowledge of dinoflagellate biogeography. This would enable further comparison of temperature changes between the Northern and Southern Hemispheres, and permit analysis of the evolution of latitudinal temperature gradients. It would also be useful to obtain more data with a higher temporal resolution to analyse shorter events, such as the MMCO, rather than solely the long term trends. It is equally important to add further quantitative records to the TOPIS database to facilitate the detection of more refined temperature changes. However, this study unequivocally demonstrates that it is possible to use dinoflagellate cysts to determine large-scale climate changes through the Neogene.

Acknowledgments

This research was jointly funded by the British Geological Survey (BGS) University Funding Initiative (BUFI) and the University of Leeds. The BGS contract number was GA/12S/004, and the BUFI reference was S227. James B. Riding publishes with the approval of the Executive Director, British Geological Survey (NERC). Ruza F. Ivanovic is funded by a NERC Independent Research Fellowship (#NE/K008536/1). Stijn De Schepper is funded by the Norwegian Research Council (project 229819). Finally, we extend our sincere thanks to the journal editor and to two anonymous reviewers whose perceptive comments and critiques helped us to significantly improve the manuscript.

Figure captions

Figure 1: Example screen shot from the Microsoft Access database; Tertiary Oceanic Parameters Information System (TOPIS) showing the three key forms: Main, Layer and Flora.

Figure 2: Distribution of all the Neogene records used in this study; the sites are plotted at their modern latitude and longitude, and references are provided in supplementary information B.

Figure 3: Age ranges of the Neogene dinoflagellate cyst species with known temperature preferences used in this study. Dashed lines represent ages when species are known to have lived, but are not present in the datasets used in this study. References pertaining to temperature preferences are provided in the Supplementary data A.

Figure 4: Distribution of dinoflagellate cyst records in (a) Aquitanian, (b) Burdigalian, (c) Langhian, (d) Serravallian, (e) Tortonian, (f) Messinian, (g) Zanclean, (h) Piacenzian and the (i) modern (from Zonneveld et al., 2013b). (j) Mean annual sea surface temperature observed between 2009 and 2013 (from NASA's Ocean Color database: http://oceancolor.gsfc.nasa.gov; NASA Ocean Biology OB.DAAC; 2014). For a-i, records are plotted at their palaeo-latitude and -longitudes. Size of the points represents the number of Cold Water Species (CWS) present in each record. The colour of the points represents the percentage of CWS relative to the total number of species with known temperature preferences present in each record. Darker shades represent higher percentages of CWS. Small red circles represent records that only contain Warm Water Species.

Figure 5: Dinoflagellate cyst data for the entire Neogene is divided into latitudinal bins spanning five degrees. There are consistently more data for the Northern Hemisphere than the Southern Hemisphere. For each record, the percentage of CWS was calculated relative to the number of species with known temperature preferences. The percentage of CWS is displayed and is represented by the horizontal thickness of the line. The shading of the lines represents the number of records present within each latitudinal bin. Dashed red lines represent records with no CWS. Figure 5a represents all records and Figure 5b contains only those records with no CWS present. Arrows indicate the two main periods of cooling. To help explore uncertainties, the number of records found within each latitudinal bin is represented by the shading. The darker the shading, the more data are present, and therefore the more reliable the signal is likely to be.

Figure 6: Mean percentages of Cold Water Species (CWS) of dinoflagellate cysts for each stage for (a) all records, (b) only records from the Northern Hemisphere and using only the latitudinal bins (in the Northern Hemisphere) where data are available for all stages. (c) Benthic $\delta^{18}O$ compilation (Zachos et al., 2001; 2008) demonstrating cooling through the Neogene to present for comparison with the mean percentage of CWS.

Figure 7: The mean percentage of Cold Water Species (CWS) of dinoflagellate cysts relative to the total number of species present with known temperature preferences for each five degree latitudinal bin. (a) Aquitanian, (b) Burdigalian, (c) Langhian, (d) Serravallian, (e) Tortonian, (f) Messinian, (g) Zanclean, (h) Piacenzian and (i) the modern. For the modern, results were replotted without data from the Gulf of St. Lawrence (grey dotted), a densely sampled region, to investigate sampling bias. This grey dotted line is included in all stages for comparison. Error bars represent the standard deviation.

Figure 8: The number of dinoflagellate cyst species with warm or cold water preferences for each stage (red and blue lines; plotted on the left axis) and the percentage of Cold Water Species (CWS) that make up the total number of species with known temperature preferences for each stage (black line; plotted on the right axis). The data were obtained by counting the number of species in each stage from the range chart in Figure 3.

Figure 9: The average age range of dinoflagellate cyst records for each stage. Generally, temporal resolution of the data is higher in shorter stages because much of the data are dated to within a stage.

Supplementary data A: A list of the species with known temperature preferences used in this study and the references from which the information came.

829 **Supplementary data B:** A list of the localities used in this study and the publications from which the

830 information came.

831

832

833 **References**

834 Abels, H., Hilgen, F., Krijgsman, W., Kruk, R., Raffi, I., Turco, E., Zachariasse, W., 2005. Long-period
835 orbital control on middle Miocene global cooling: Integrated stratigraphy and astronomical
836 tuning of the Blue Clay Formation on Malta. Paleoceanography 20, PA4012, doi:
837 10.1029/2004PA001129.

838 Badger, M.P., Lear, C.H., Pancost, R.D., Foster, G.L., Bailey, T.R., Leng, M.J., Abels, H.A., 2013. CO_2
839 drawdown following the middle Miocene expansion of the Antarctic Ice Sheet.
840 Paleoceanography 28, 42–53.

841 Bailey, I., Hole, G.M., Foster, G.L., Wilson, P.A., Storey, C.D., Trueman, C.N., Raymo, M.E., 2013. An
842 alternative suggestion for the Pliocene onset of major northern hemisphere glaciation based
843 on the geochemical provenance of North Atlantic Ocean ice-rafted debris. Quaternary
844 Science Reviews 75, 181–194.

845 Balco, G., Rovey, C.W., 2010, Absolute chronology for major Pleistocene advances of the Laurentide
846 Ice Sheet: Geology 38, 795–798, DOI: 10.1130/G30946.1.

847 Banks, R., 1966. The cold layer in the Gulf of St. Lawrence. Journal of Geophysical Research 71,
848 1603–1610.

849 Beddow, H.M., Liebrand, D., Sluijs, A., Wade, B.S., Lourens, L.J., 2016. Global change across the
850 Oligocene-Miocene transition: High-resolution stable isotope records from IODP Site U1334
851 (equatorial Pacific Ocean). Paleoceanography 31, 81–97.

852 Beerling, D.J., Royer, D.L., 2011. Convergent cenozoic CO2 history. *Nature Geoscience,* 4, 418–420.

853 Benson, R.B., Butler, R.J., Lindgren, J., Smith, A.S., 2009. Mesozoic marine tetrapod diversity: mass
854 extinctions and temporal heterogeneity in geological megabiases affecting vertebrates.
855 Proceedings of the Royal Society of London 277, 829–834.

856 Billups, K., Schrag, D., 2002. Paleotemperatures and ice volume of the past 27 Myr revisited with
857 paired Mg/Ca and 18O/16O measurements on benthic foraminifera. Paleoceanography 17,
858 1003–1014.

Bockelmann, F.D., Zonneveld, K.A., Schmidt, M., 2007. Assessing environmental control on dinoflagellate cyst distribution in surface sediments of the Benguela upwelling region (eastern South Atlantic). *Limnology and Oceanography*, 52, 2582–2594.

Bogus, K., Harding, I.C., King, A., Charles, A.J., Zonneveld, K.A., Versteegh, G.J., 2012. The composition and diversity of dinosporin in species of the *Apectodinium* complex (Dinoflagellata). Review of Palaeobotany and Palynology 183**,** 21–31.

Bogus, K., Mertens, K.N., Lauwaert, J., Harding, I.C., Vrielinck, H., Zonneveld, K.A., Versteegh, G.J., 2014. Differences in the chemical composition of organic-walled dinoflagellate resting cysts from phototrophic and heterotrophic dinoflagellates. Journal of phycology 50**,** 254–266.

Böhme, M., 2003. The Miocene climatic optimum: evidence from ectothermic vertebrates of Central Europe. Palaeogeography, Palaeoclimatology, Palaeoecology 195, 389–401.

Bojar, A.-V., Hiden, H., Fenninger, A., Neubauer, F., 2004. Middle Miocene seasonal temperature changes in the Styrian basin, Austria, as recorded by the isotopic composition of pectinid and brachiopod shells. Palaeogeography, Palaeoclimatology, Palaeoecology 203, 95–105.

Bolton, C.T., Stoll, H.M., 2013. Late Miocene threshold response of marine algae to carbon dioxide limitation. Nature 500, 558–562.

Bonnet, S., de Vernal, A., Gersonde, R., Lembke-Jene, L., 2012. Modern distribution of dinocysts from the North Pacific Ocean (37–64 N, 144 E–148 W) in relation to hydrographic conditions, sea-ice and productivity. Marine Micropaleontology 84, 87–113.

Bradshaw, C.D.C., Lunt, D.J., Flecker, R., Salzmann, U., Pound, M.J., Haywood, A.M., Eronen, J.T., 2012. The relative roles of CO2 and palaeogeography in determining Late Miocene climate: results from a terrestrial model-data comparison. Climate of the Past 8, 1257–1285.

Bradshaw, C.D., Lunt, D.J., Flecker, R., Davies-Barnard, T., 2015. Disentangling the roles of Late Miocene palaeogeography and vegetation – Implications for climate sensitivity. Palaeogeography, Palaeoclimatology, Palaeoecology 417, 17–34.

884 Brierley, C.M., Fedorov, A.V., 2010. Relative importance of meridional and zonal sea surface
885 temperature gradients for the onset of the ice ages and Pliocene-Pleistocene climate
886 evolution. Paleoceanography 25, doi: 10.1029/2009PA001809.
887 Brierley, C.M., Fedorov, A.V., 2016. Comparing the impacts of Miocene–Pliocene changes in inter-
888 ocean gateways on climate: Central American Seaway, Bering Strait, and Indonesia. Earth
889 and Planetary Science Letters 444, 116–130.
890 Brinkhuis, H., Bujak, J., Smit, J., Versteegh, G., Visscher, H., 1998. Dinoflagellate-based sea surface
891 temperature reconstructions across the Cretaceous–Tertiary boundary. Palaeogeography,
892 Palaeoclimatology, Palaeoecology 141, 67–83.
893 Bruch, A., Utescher, T., Mosbrugger, V., Gabrielyan, I., Ivanov, D., 2006. Late Miocene climate in the
894 circum-Alpine realm—a quantitative analysis of terrestrial palaeofloras. Palaeogeography,
895 Palaeoclimatology, Palaeoecology 238, 270–280.
896 Butler, R.J., Benson, R.B., Carrano, M.T., Mannion, P.D., Upchurch, P., 2011. Sea level, dinosaur
897 diversity and sampling biases: investigating the 'common cause' hypothesis in the terrestrial
898 realm. Proceedings of the Royal Society of London B: Biological Sciences 278, 1165–1170.
899 Coates, A.G., Stallard, R.F., 2013. How old is the Isthmus of Panama? Bulletin of Marine Science 89,
900 801–813.
901 Crame, J.A., 2001. Taxonomic diversity gradients through geological time. Diversity and Distributions
902 7, 175–189.
903 Crouch, E.M., Dickens, G.R., Brinkhuis, H., Aubry, M.-P., Hollis, C.J., Rogers, K.M., Visscher, H., 2003.
904 The *Apectodinium* acme and terrestrial discharge during the Paleocene–Eocene thermal
905 maximum: new palynological, geochemical and calcareous nannoplankton observations at
906 Tawanui, New Zealand. Palaeogeography, Palaeoclimatology, Palaeoecology 194, 387–403.
907 Crowley, T.J., 2000. Carbon dioxide and Phanerozoic climate. Warm Climates in Earth History.
908 Cambridge University Press Cambridge, 425–444.

909 Dale, B., 1983. Dinoflagellate resting cysts: “benthic plankton”. In: Fryxell, G.A. (editor). Survival
910 strategies of the algae. Cambridge University Press, 69–136.
911 Dale, B., 1996. Dinoflagellate cyst ecology: modeling and geological applications. In: Jansonius, J.,
912 McGregor, D.C. (editors). Palynology: principles and applications. American Association of
913 Stratigraphic Palynologists Foundation, Dallas 3, 1249–1275.
914 DeConto, R.M., Pollard, D., Wilson, P.A., Pälike, H., Lear, C.H., Pagani, M., 2008. Thresholds for
915 Cenozoic bipolar glaciation. Nature 455, 652-656.
916 Denk, T., Grimm, G.W., Grímsson, F., Zetter, R., 2013. Evidence from "Köppen signatures" of fossil
917 plant assemblages for effective heat transport of Gulf Stream to subarctic North Atlantic
918 during Miocene cooling. Biogeosciences 10, 7927–7942.
919 De Schepper, S., Fischer, E.I., Groeneveld, J., Head, M.J., Matthiessen, J., 2011. Deciphering the
920 palaeoecology of Late Pliocene and Early Pleistocene dinoflagellate cysts. Palaeogeography,
921 Palaeoclimatology, Palaeoecology 309, 17–32.
922 De Schepper, S., Gibbard, P.L., Salzmann, U., Ehlers, J., 2014. A global synthesis of the marine and
923 terrestrial evidence for glaciation during the Pliocene Epoch. Earth-Science Reviews 135, 83–
924 102.
925 De Schepper, S., Head, M.J., Groeneveld, J., 2009. North Atlantic Current variability through marine
926 isotope stage M2 (circa 3.3 Ma) during the mid-Pliocene. Paleoceanography 24.
927 De Schepper, S., Head, M.J., Louwye, S., 2004. New dinoflagellate cyst and *incertae sedis* taxa from
928 the Pliocene of northern Belgium, southern North Sea Basin. Journal of Paleontology 78,
929 625–644.
930 De Schepper, S., Schreck, M., Beck, K.M., Matthiessen, J., Fahl, K., Mangerud, G., 2015. Early Pliocene
931 onset of modern Nordic Seas circulation related to ocean gateway changes. Nature
932 Communications 6, doi: 10.1038/ncomms9659
933 de Vernal, A., Marret, F., 2007. Organic-walled dinoflagellate cysts: tracers of sea-surface conditions.
934 Developments in Marine Geology 1, 371–408, Elsevier B.V.

de Vernal, A., Rochon, A., Fréchette, B., Henry, M., Radi, T., Solignac, S., 2013. Reconstructing past sea ice cover of the Northern Hemisphere from dinocyst assemblages: status of the approach. Quaternary Science Reviews 79, 122–134.

de Verteuil, L., Norris, G., 1996. Miocene Dinoflagellate stratigraphy and systematics of Maryland and Virginia. Micropaleontology 42, 1–82.

Diester-Haass, L., Meyers, P.A., Rothe, P., 1990. Miocene history of the Benguela Current and Antarctic ice volumes: Evidence from rhythmic sedimentation and current growth across the Walvis Ridge (Deep Sea Drilling Project Sites 362 and 532). Paleoceanography 5, 685–707.

Dolan, A.M., Haywood, A.M., Hill, D.J., Dowsett, H.J., Hunter, S.J., Lunt, D.J., Pickering, S.J., 2011. Sensitivity of Pliocene ice sheets to orbital forcing. Palaeogeography, Palaeoclimatology, Palaeoecology 309, 98–110.

Donders, T., Weijers, J., Munsterman, D., Kloosterboer-Van Hoeve, M., Buckles, L., Pancost, R., Schouten, S., Damsté, J. S., Brinkhuis, H., 2009. Strong climate coupling of terrestrial and marine environments in the Miocene of northwest Europe. Earth and Planetary Science Letters 281, 215–225.

Dowsett, H., Dolan, A., Rowley, D., Moucha, R., Forte, A.M., Mitrovica, J.X., Pound, M., Salzmann, U., Robinson, M., Chandler, M., Foley, K., Haywood, A., 2016. The PRISM4 (mid-Piacenzian) paleoenvironmental reconstruction. Climate of the Past 12, 1519–1538.

Dowsett, H.J., Foley, K.M., Stoll, D.K., Chandler, M.A., Sohl, L.E., Bentsen, M., Otto-Bliesner, B.L., Bragg, F.J., Chan, W.-L., Contoux, C., Dolan, A.M., Haywood, A.M., Jonas, J.A., Jost, A., Kamae, Y., Lohmann, G., Lunt, D.J., Nisancioglu, K.H., Abe-Ouchi, A., Ramstein, G., Riesselman, C.R., Robinson, M.M., Rosenbloom, N.A., Salzmann, U., Stepanek, C., Strother, S.L., Ueda, H., Yan, Q., Zhang, Z., 2013. Sea Surface Temperature of the mid-Piacenzian Ocean: A Data-Model Comparison. Science Reports 3.

Drury, A.J., John, C.M., Shevenell, A.E., 2016. Evaluating climatic response to external radiative forcing during the late Miocene to early Pliocene: New perspectives from eastern equatorial Pacific (IODP U1338) and North Atlantic (ODP 982) locations. Paleoceanography 31, 167-184.

Fauquette, S., Suc, J.-P., Jiménez-Moreno, G., Micheels, A., Jost, A., Favre, E., Bachiri-Taoufiq, N., Bertini, A., Clet-Pellerin, M., Diniz, F., 2007. Latitudinal climatic gradients in the Western European and Mediterranean regions from the Mid-Miocene (c. 15 Ma) to the Mid-Pliocene (c. 3.5 Ma) as quantified from pollen data. In: Williams, M., Haywood, A.M., Gregory, F.J., Schmidt, D.N., (editors). Deep-time perspectives on climate change. The Micropalaeontological Society Special Publications. The Geological Society, London, 481–502.

Fauquette, S., Bernet, M., Suc, J.-P., Grosjean, A.-S., Guillot, S., van der Beek, P., Jourdan, S., Popescu, S.-M., Jiménez-Moreno, G., Bertini, A., Pittet, B., Tricart, P., Dumont, T., Schwartz, S., Zheng, Z., Roche, E., Pavia, G., Gardien, V., 2015. Quantifying the Eocene to Pleistocene topographic evolution of the southwestern Alps, France and Italy. Earth and Planetary Science Letters 412, 220-234.

Fedorov, A.V., Brierley, C.M., Lawrence, K.T., Liu, Z., Dekens, P.S., Ravelo, A.C., 2013. Patterns and mechanisms of early Pliocene warmth. Nature 496, 43–49.

Fensome, R.A., MacRae, R.A., Williams, G.L., 2008. DINOFLAJ2, version 1. American Association of Stratigraphic Palynologists, Data Series, 1, 937p.

Fensome, R.A, Taylor, F.J.R., Norris, G., Sarjeant, W.A.S., Wharton, D.I., Williams, G.L., 1993. A classification of living and fossil dinoflagellates. American Museum of Natural History, Micropaleontology Special Publication 7. Sheridan Press, Hanover, PA. 351 p.

Flecker, R., Krijgsman, W., Capella, W., De Castro Martíns, C., Dmitrieva, E., Mayser, J.P., Marzocchi, A., Modestu, S., Ochoa, D., Simon, D., 2015. Evolution of the Late Miocene Mediterranean–

983 Atlantic gateways and their impact on regional and global environmental change. Earth-
984 Science Reviews 150, 365–392.
985 Flower, B., Kennett, J., 1993. Middle Miocene ocean-climate transition: High-resolution oxygen and
986 carbon isotopic records from Deep Sea Drilling Project Site 588A, southwest Pacific.
987 Paleoceanography 8, 811–843.
988 Flower, B.P., Kennett, J.P., 1994. The middle Miocene climatic transition: East Antarctic ice sheet
989 development, deep ocean circulation and global carbon cycling. Palaeogeography,
990 Palaeoclimatology, Palaeoecology 108, 537–555.
991 Forrest, M., Eronen, J.T., Utescher, T., Knorr, G. , Stepanek, C., Lohmann, G., Hickler, T., 2015.
992 Climate-vegetation modelling and fossil plant data suggest low atmospheric CO_2 in the Late
993 Miocene. Climate of the Past 11, 1701–1732.
994 Foster, G.L., Lear, C.H., Rae, J.W., 2012. The evolution of pCO_2, ice volume and climate during the
995 middle Miocene. Earth and Planetary Science Letters 341, 243–254.
996 Gibbard, P.L., Head, M.J., Walker, M.J.C., 2010. Formal ratification of the Quaternary System/Period
997 and the Pleistocene Series/Epoch with a base at, 2.58 Ma. Journal of Quaternary Science 25,
998 96–102.
999 Gradstein, F.M., Ogg, G., Schmitz, M., 2012. The Geologic Time Scale 2012, Amsterdam, Elsevier, 2-
1000 Volume Set, 1144 p.
1001 Graham, A., 2009. The Andes: A geological overview from a biological perspective. Annals of the
1002 Missouri Botanical Garden 96, 371-385.
1003 Greenop, R., Foster, G.L., Wilson, P.A., Lear, C.H., 2014. Middle Miocene climate instability
1004 associated with high-amplitude CO_2 variability. Paleoceanography 29, 845-853.
1005 Grunert, P., Tzanova, A., Harzhauser, M., Piller, W.E., 2014. Mid-Burdigalian Paratethyan alkenone
1006 record reveals link between orbital forcing, Antarctic ice-sheet dynamics and European
1007 climate at the verge to Miocene Climate Optimum. Global and Planetary Change 123, 36–43.

1008 Hansen, J., Sato, M., Russell, G., Kharecha, P., 2013. Climate sensitivity, sea level and atmospheric
1009 carbon dioxide. Philosophical Transactions of the Royal Society of London A: Mathematical,
1010 Physical and Engineering Sciences 371, doi: 10.1098/rsta.2012.0294.
1011 Harland, R., 1983. Distribution maps of recent dinoflagellate cysts in bottom sediments from the
1012 North-Atlantic Ocean and adjacent seas. Palaeontology 26, 321–387.
1013 Harland, R., Pudsey, C.J., 1999. Dinoflagellate cysts from sediment traps deployed in the
1014 Bellingshausen, Weddell and Scotia seas, Antarctica. *Marine Micropaleontology*, 37, 77–99.
1015 Haywood, A., Hill, D., Dolan, A., Otto-Bliesner, B., Bragg, F., Chan, W.-L., Chandler, M., Contoux, C.,
1016 Dowsett, H., Jost, A., 2013. Large-scale features of Pliocene climate: results from the
1017 Pliocene Model Intercomparison Project. Climate of the Past 9, 191–209.
1018 Haywood, A.M., Dowsett, H.J., Dolan, A.M., Rowley, D., Abe-Ouchi, A., Otto-Bliesner, B., Chandler,
1019 M.A., Hunter, S.J., Lunt, D.J., Pound, M., Salzmann, U., 2016. The Pliocene Model
1020 Intercomparison Project (PlioMIP) Phase 2: scientific objectives and experimental design.
1021 Climate of the Past 12, 663–675.
1022 Haywood, A.M., Valdes, P.J., Sellwood, B.W., 2002. Magnitude of climate variability during middle
1023 Pliocene warmth: a palaeoclimate modelling study. Palaeogeography, Palaeoclimatology,
1024 Palaeoecology 188, 1–24.
1025 Head, M.J., Norris, G., Mudie, P.J., 1989. New species of dinocysts and a new species of acritarch
1026 from the upper Miocene and lowermost Pliocene, ODP Leg 105, Site 646, Labrador Sea.
1027 Proceedings of the Ocean Drilling Program 105, 453–466.
1028 Head, M.J., 1994. Morphology and paleoenvironmental significance of the Cenozoic dinoflagellate
1029 genera *Tectatodinium* and *Habibacysta*. Micropaleontology 40, 289–321.
1030 Head, M.J., 1997. Thermophilic dinoflagellate assemblages from the mid Pliocene of eastern
1031 England. Journal of Paleontology 71, 165–193.
1032 Heinrich, S., Zonneveld, K.A., Bickert, T., Willems, H., 2011. The Benguela upwelling related to the
1033 Miocene cooling events and the development of the Antarctic Circumpolar Current:

1034 Evidence from calcareous dinoflagellate cysts. Paleoceanography 26, doi:
1035 10.1029/2010PA002065.
1036 Hennissen, J.A., Head, M.J., De Schepper, S., Groeneveld, J., 2014. Palynological evidence for a
1037 southward shift of the North Atlantic Current at~ 2.6 Ma during the intensification of late
1038 Cenozoic Northern Hemisphere glaciation. Paleoceanography 29, 564–580.
1039 Hennissen, J.A., Head, M.J., De Schepper, S. and Groeneveld, J., 2017. Dinoflagellate cyst
1040 paleoecology during the Pliocene–Pleistocene climatic transition in the North Atlantic.
1041 Palaeogeography, Palaeoclimatology, Palaeoecology 470, 81–108.
1042 Herbert, T.D., Lawrence, K.T., Tzanova, A., Peterson, L.C., Caballero-Gill, R., Kelly, C.S., 2016, Late
1043 Miocene global cooling and the rise of modern ecosystems: Nature Geoscience 9, 843-847.
1044 Hoetzel, S., Dupont, L.M., Wefer, G., 2015. Miocene–Pliocene vegetation change in south-western
1045 Africa (ODP Site 1081, offshore Namibia). Palaeogeography, Palaeoclimatology,
1046 Palaeoecology 423, 102–108.
1047 Hopkins, J.A., McCarthy, F.M.G., 2002. Post-depositional palynomorph degradation in Quaternary
1048 shelf sediments: A laboratory experiment studying the effects of progressive oxidation.
1049 Palynology 26, 167–184.
1050 Hunter, S.J., Haywood, A.M., Valdes, P.J., Francis, J.E., Pound, M.J., 2013. Modelling equable climates
1051 of the Late Cretaceous: Can new boundary conditions resolve data–model discrepancies?
1052 Palaeogeography, Palaeoclimatology, Palaeoecology 392, 41–51.
1053 Ivanovic, R.F., Valdes, P.J., Flecker, R. and Gutjahr, M., 2014. Modelling global-scale climate impacts
1054 of the late Miocene Messinian Salinity Crisis. Climate of the Past, 10, 607–622.
1055 Jablonski, D., Roy, K., Valentine, J.W., Price, R.M., Anderson, P.S., 2003. The impact of the pull of the
1056 recent on the history of marine diversity. Science 300, 1133–1135.
1057 Jansen, E., Bleil, U., Henrich, R., Kringstad, L., Slettemark, B., 1988, Paleoenvironmental changes in
1058 the Norwegian Sea and the northeast Atlantic during the last 2.8 Ma: Deep Sea Drilling
1059 Project/Ocean Drilling Program ites 610, 642, 643 and 644: Paleoceanography 3, 563–581.

1060 Karas, C., Nürnberg, D., Bahr, A., Groeneveld, J., Herrle, J.O., Tiedemann, R., 2017. Pliocene oceanic
1061 seaways and global climate. Scientific Reports 7, 39842.
1062 Kawamura, H., 2004. Dinoflagellate cyst distribution along a shelf to slope transect of an oligotrophic
1063 tropical sea (Sunda Shelf, South China Sea). Phycological Research 52, 355–375.
1064 Knorr, G., Butzin, M., Micheels, A., Lohmann, G., 2011. A warm Miocene climate at low atmospheric
1065 CO_2 levels. Geophysical Research Letters 38, doi: 10.1029/2011GL048873.
1066 Knorr, G., Lohmann, G., 2014. Climate warming during Antarctic ice sheet expansion at the Middle
1067 Miocene transition. Nature Geoscience 7, 376-381.
1068 Kroh, A., 2007. Climate changes in the Early to Middle Miocene of the Central Paratethys and the
1069 origin of its echinoderm fauna. Palaeogeography, Palaeoclimatology, Palaeoecology 253,
1070 169–207.
1071 Kürschner, W.M., Kvaček, Z., Dilcher, D.L., 2008. The impact of Miocene atmospheric carbon dioxide
1072 fluctuations on climate and the evolution of terrestrial ecosystems. Proceedings of the
1073 National Academy of Sciences 105, 449–453.
1074 Larsen, H.C., Saunders, A.D., Clift, P.D., Beget, J., Wei, W., Spezzaferri, S., 1994. Seven Million Years
1075 of Glaciation in Greenland. Science 264, 952-954.
1076 Lear, C.H., Coxall, H.K., Foster, G.L., Lunt, D.J., Mawbey, E.M., Rosenthal, Y., Sosdian, S.M., Thomas,
1077 E., Wilson, P.A., 2015. Neogene ice volume and ocean temperatures: Insights from infaunal
1078 foraminiferal Mg/Ca paleothermometry. Paleoceanography 30, 1437–1454.
1079 Liebrand, D., de Bakker, A.T.M., Beddow, H.M., Wilson, P.A., Bohaty, S.M., Ruessink, G., Pälike, H.,
1080 Batenburg, S.J., Hilgen, F.J., Hodell, D.A., Huck, C.E., Kroon, D., Raffi, I., Saes, M.J.M., van Dijk,
1081 A.E., Lourens, L.J., 2017. Evolution of the early Antarctic ice ages. Proceedings of the
1082 National Academy of Sciences 114, 3867–3872.
1083 Limoges, A., Londeix, L., de Vernal, A., 2013. Organic-walled dinoflagellate cyst distribution in the
1084 Gulf of Mexico. Marine Micropaleontology 102, 51–68.

1085 Lisiecki, L.E., Raymo, M.E., 2005. A Pliocene-Pleistocene stack of 57 globally distributed benthic $\delta^{18}O$
1086 records. Paleoceanography 20, doi: 10.1029/2004PA001071.
1087 Long, Z., Perrie, W., Chassé, J., Brickman, D., Guo, L., Drozdowski, A., Hu, H., 2015. Impacts of climate
1088 change in the Gulf of St. Lawrence. Atmosphere-Ocean 54, 1–15.
1089 Londeix, L., Jan du Chêne, R., 1998. Burdigalian dinocyst stratigraphy of the stratotypic area
1090 (Bordeaux, France). Geobios 31, 283–294.
1091 Louwye, S., De Coninck, J., Verniers, J., 2000. Shallow marine Lower and Middle Miocene deposits at
1092 the southern margin of the North Sea Basin (northern Belgium): dinoflagellate cyst
1093 biostratigraphy and depositional history. Geological Magazine 137, 381–394.
1094 Louwye, S., De Schepper, S., Laga, P., Vandenberghe, N., 2007. The upper Miocene of the southern
1095 North Sea Basin (northern Belgium): a palaeoenvironmental and stratigraphical
1096 reconstruction using dinoflagellate cysts. Geological Magazine 144, 33–52.
1097 Louwye, S., De Schepper, S., 2010. The Miocene–Pliocene hiatus in the southern North Sea Basin
1098 (northern Belgium) revealed by dinoflagellate cysts. Geological Magazine 147, 760–776.
1099 Lunt, D.J., Valdes, P.J., Haywood, A., Rutt, I.C., 2008. Closure of the Panama Seaway during the
1100 Pliocene: implications for climate and Northern Hemisphere glaciation. Climate
1101 Dynamics, *30*, 1–18.
1102 Mannion, P.D., Upchurch, P., Benson, R.B., Goswami, A., 2014. The latitudinal biodiversity gradient
1103 through deep time. Trends in Ecology and Evolution 29, 42–50.
1104 Markwick, P.J., Rowley, D.B., Ziegler, A.M., Hulver, M.L., Valdes, P.J., Sellwood, B.W., 2000. Late
1105 Cretaceous and Cenozoic global palaeogeographies: Mapping the transition from a “hot-
1106 house” to an “ice-house” world. Geologiska i Stockholm Gorehandlingar 122, 103 p.
1107 Marret, F., 1993. Les effets de l'acétolyse sur les assemblages des kystes de dinoflagellés.
1108 Palynosciences 2, 267–272.
1109 Marret, F., Zonneveld, K.A., 2003. Atlas of modern organic-walled dinoflagellate cyst distribution.
1110 Review of Palaeobotany and Palynology 125, 1–200.

1111 Masure, E., Aumar, A.-M., Vrielynck, B., 2013. Worldwide palaeogeography of Aptian and Late Albian
1112 dinoflagellate cysts: Implications for sea-surface temperature gradients and palaeoclimate.
1113 In: Lewis, J.M., Marret, F., Bradley, L., (editors). Biological and Geological Perspectives of
1114 Dinoflagellates. The Micropalaeontological Society, Special Publications. Geological Society,
1115 London, 97–125.
1116 Masure, E., Vrielynck, B., 2009. Late Albian dinoflagellate cyst paleobiogeography as indicator of
1117 asymmetric sea surface temperature gradient on both hemispheres with southern high
1118 latitudes warmer than northern ones. Marine Micropaleontology 70, 120–133.
1119 McCarthy, F.M., Mudie, P.J., 1996. Palynology and dinoflagellate biostratigraphy of upper Cenozoic
1120 sediments from Sites 898 and 900, Iberia Abyssal Plain. Proceedings of the Ocean Drilling
1121 Program, Scientific Results 149, 241–265.
1122 McKay, R., Naish, T., Carter, L., Riesselman, C., Dunbar, R., Sjunneskog, C., Winter, D., Sangiorgi, F.,
1123 Warren, C., Pagani, M., 2012. Antarctic and Southern Ocean influences on Late Pliocene
1124 global cooling. Proceedings of the National Academy of Sciences 109, 6423–6428.
1125 Mertens, K.N., Takano, Y., Head, M.J., Matsuoka, K., 2014. Living fossils in the Indo-Pacific warm
1126 pool: A refuge for thermophilic dinoflagellates during glaciations. Geology 42, 531–534.
1127 Mertens, K.N., Verhoeven, K., Verleye, T., Louwye, S., Amorim, A., Ribeiro, S., Deaf, A.S., Harding,
1128 I.C., De Schepper, S., González, C., Kodrans-Nsiah, M., de Vernal, A., Henry, M., Radi, T.,
1129 Dybkjær, K., Poulsen, N.E., Feist-Burkhardt, S., Chitolie, J., Heilmann-Clausen, C., Londeix, L.,
1130 Turon, J.-L., Marret, F., Matthiessen, J., McCarthy, F.M.G., Prasad, V., Pospelova, V., Kyffin-
1131 Hughes, J.E., Riding, J.B., Rochon, A., Sangiorgi, F., Welters, N., Sinclair, N., Thun, C., Soliman,
1132 A., van Nieuwenhove, N., Vink, A., Young, M., 2009. Determining the absolute abundance of
1133 dinoflagellate cysts in recent marine sediments: The *Lycopodium* marker-grain method put
1134 to the test. Review of Palaeobotany and Palynology 157, 238–252.

1135 Miao, Y., Herrmann, M., Wu, F., Yan, X., Yang, S., 2012. What controlled Mid–Late Miocene long-
1136 term aridification in Central Asia?—Global cooling or Tibetan Plateau uplift: A review. Earth-
1137 Science Reviews 112, 155–172.
1138 Miller, K.G., Wright, J.D., Fairbanks, R.G., 1991. Unlocking the icehouse: Oligocene–Miocene oxygen
1139 isotopes, eustacy and margin erosion, Journal of Geophysical Research 96, 6829–6848.
1140 Miller, K.G., Kominz, M.A., Browning, J.V., Wright, J.D., Mountain, G.S., Katz, M.E., Sugarman, P.J.,
1141 Cramer, B.S., Christie-Blick, N., Pekar, S.F., 2005. The Phanerozoic record of global sea-level
1142 change. Science 310, 1293–1298.
1143 Miller, K.G., Wright, J.D., Browning, J.V., Kulpecz, A., Kominz, M., Naish, T.R., Cramer, B.S., Rosenthal,
1144 Y., Peltier, W.R., Sosdian, S., 2012. High tide of the warm Pliocene: Implications of global sea
1145 level for Antarctic deglaciation. Geology 40, 407–410.
1146 Mittelbach, G.G., Schemske, D.W., Cornell, H.V., Allen, A.P., Brown, J.M., Bush, M.B., Harrison, S.P.,
1147 Hurlbert, A.H., Knowlton, N., Lessios, H.A., 2007. Evolution and the latitudinal diversity
1148 gradient: speciation, extinction and biogeography. Ecology Letters 10, 315–331.
1149 Montes, C., Cardona, A., Jaramillo, C., Pardo, A., Silva, J.C., Valencia, V., Ayala, C., Pérez-Angel, L.C.,
1150 Rodriguez-Parra, L.A., Ramirez, V., Niño, H., 2015. Middle Miocene closure of the Central
1151 American Seaway. Science 348, 226–229.
1152 Moran, K., Backman, J., Brinkhuis, H., Clemens, S.C., Cronin, T., Dickens, G.R., Eynaud, F., Gattacceca,
1153 J., Jakobsson, M., Jordan, R.W., Kaminski, M., King, J., Koc, N., Krylov, A., Martinez, N.,
1154 Matthiessen, J., McInroy, D., Moore, T.C., Onodera, J., O'Regan, M., Pälike, H., Rea, B., Rio,
1155 D., Sakamoto, T., Smith, D.C., Stein, R., St John, K., Suto, I., Suzuki, N., Takahashi, K.,
1156 Watanabe, M., Yamamoto, M., Farrell, J., Frank, M., Kubik, P., Jokat, W., Kristoffersen, Y.,
1157 2006. The Cenozoic palaeoenvironment of the Arctic Ocean. Nature 441, 601–605.
1158 Mudelsee, M., Raymo, M.E., 2005. Slow dynamics of the Northern Hemisphere glaciation.
1159 Paleoceanography 20, doi: 1 0.1029/2005PA001153.

1160 Mudie, P.J., McCarthy, F.M., 2006. Marine palynology: potentials for onshore—offshore correlation
1161 of Pleistocene-Holocene records. Transactions of the Royal Society of South Africa 61**,** 139–
1162 157.
1163 Naish, T.R., Wilson, G.S., 2009. Constraints on the amplitude of Mid-Pliocene (3.6–2.4 Ma) eustatic
1164 sea-level fluctuations from the New Zealand shallow-marine sediment record. Philosophical
1165 Transactions of the Royal Society of London A: Mathematical, Physical and Engineering
1166 Sciences 367, 169–187.
1167 NASA Ocean Biology (OB.DAAC), 2014. Mean annual sea surface temperature for
1168 the period 2009–2013 (composite dataset created by UNEP-WCMC). Data obtained
1169 from the Moderate Resolution Imaging Spectroradiometer (MODIS) Aqua Ocean
1170 Colour website (NASA OB.DAAC, Greenbelt, MD, USA). Accessed 28/11/2014. URL:
1171 http://oceancolor.gsfc.nasa.gov/cgi/l3. Cambridge (UK): UNEP World Conservation
1172 Monitoring Centre. URL: http://data.unep-wcmc.org/datasets/36.
1173 Nikolaev, S., Oskina, N., Blyum, N., Bubenshchikova, N., 1998. Neogene–Quaternary variations of the
1174 Pole–Equator temperature gradient of the surface oceanic waters in the North Atlantic and
1175 North Pacific. Global and Planetary Change 18, 85–111.
1176 Osbourne, A.H., Newkirk, D.R., Groeneveld, J., Martin, E.E., Tiedemann, R., Frank, M., 2014. The
1177 seawater neodymium and lead isotope record of the final stages of Central American Seaway
1178 closure. Paleoceanography 29, pp.715–729.
1179 Pagani, M., Arthur, M.A., Freeman, K.H., 1999. Miocene evolution of atmospheric carbon dioxide.
1180 Paleoceanography 14, 273–292.
1181 Pagani, M., Zachos, J.C., Freeman, K.H., Tipple, B., Bohaty, S., 2005. Marked decline in atmospheric
1182 carbon dioxide concentrations during the Paleogene. Science 309, 600–603.

1183 Panitz, S., Salzmann, U., Risebrobakken, B., De Schepper, S., Pound, M.J., 2016. Climate variability
1184 and long-term expansion of peat lands in Arctic Norway during the late Pliocene (ODP Site
1185 642, Norwegian Sea). Climate of the Past 12(4), 1043–1060, doi: 10.5194/cp-12-1043-2016.

1186 Pearson, P.N., Palmer, M.R., 2000. Atmospheric carbon dioxide concentrations over the past 60
1187 million years. Nature 406, 695–699.
1188 Pospelova, V., de Vernal, A., Pedersen, T.F., 2008. Distribution of dinoflagellate cysts in surface
1189 sediments from the northeastern Pacific Ocean (43–25 N) in relation to sea-surface
1190 temperature, salinity, productivity and coastal upwelling. Marine Micropaleontology 68, 21–
1191 48.
1192 Potter, P.E., Szatmari, P., 2009. Global Miocene tectonics and the modern world. Earth–Science
1193 Reviews 96, 279–295.
1194 Pound, M.J., Haywood, A.M., Salzmann, U., Riding, J.B., Lunt, D.J., Hunter, S.J., 2011. A Tortonian
1195 (Late Miocene, 11.61–7.25 Ma) global vegetation reconstruction. Palaeogeography,
1196 Palaeoclimatology, Palaeoecology 300, 29–45.
1197 Pound, M.J., Haywood, A.M., Salzmann, U., Riding, J.B., 2012a. Global vegetation dynamics and
1198 latitudinal temperature gradients during the Mid to Late Miocene (15.97–5.33 Ma). Earth-
1199 Science Reviews 112, 1–22.
1200 Pound, M.J., Riding, J.B., Donders, T.H., Daskova, J., 2012b. The palynostratigraphy of the
1201 Brassington Formation (Upper Miocene) of the southern Pennines, central England.
1202 Palynology 36, 26–37.
1203 Pound, M.J., Lowther, R.I., Peakall, J., Chapman, R.J., Salzmann, U., 2015. Palynological evidence for a
1204 warmer boreal climate in the Late Pliocene of the Yukon Territory, Canada. Palynology 39,
1205 91-102.

1206 Pound, M.J., Riding, J.B., 2016. Palaeoenvironment, palaeoclimate and age of the Brassington
1207 Formation (Miocene) of Derbyshire, UK. Journal of the Geological Society 173, 306–319.

1208 Pound, M.J., Salzmann, U., 2017. Heterogeneity in global vegetation and terrestrial climate change
1209 during the late Eocene to early Oligocene transition. Scientific Reports 7, 43386.

1210 Prebble, J.G., Reichgelt, T., Mildenhall, D.C., Greenwood, D.R., Raine, J.I., Kennedy, E.M., Seebeck,
1211 H.C., 2017. Terrestrial climate evolution in the Southwest Pacific over the past 30 million
1212 years. Earth and Planetary Science Letters 459, 136–144.

1213 Pudsey, C.J., Harland, R., 2001. Data Report: Dinoflagellate cyst analysis of Neogene sediments from
1214 Sites 1095 and 1096, Antarctic Peninsula Continental Rise. Proceedings of the Ocean Drilling
1215 Program 178, 1–10.

1216 Quaijtaal, W., Donders, T.H., Persico, D., Louwye, S., 2014. Characterising the middle Miocene Mi-
1217 events in the Eastern North Atlantic realm: A first high-resolution marine palynological
1218 record from the Porcupine Basin. Palaeogeography, Palaeoclimatology, Palaeoecology 399,
1219 140–159.

1220 Radi, T., De Vernal, A., 2008. Dinocysts as proxy of primary productivity in mid–high latitudes of the
1221 Northern Hemisphere. Marine Micropaleontology 68, 84–114.

1222 Raup, D.M., 1979. Biases in the fossil record of species and genera. Bulletin of the Carnegie Museum
1223 of Natural History 13, 85–91.

1224 Ravelo, A.C., Andreasen, D.H., Lyle, M., Lyle, A.O., Wara, M.W., 2004. Regional climate shifts caused
1225 by gradual global cooling in the Pliocene epoch. Nature 429, 263–267.

1226 Raymo, M., Ruddiman, W.F., 1992. Tectonic forcing of late Cenozoic climate. Nature 359, 117–122.

1227 Raymo, M.E., Ruddiman, W.F., Froelich, P.N., 1988. Influence of late Cenozoic mountain building on
1228 ocean geochemical cycles. Geology 16, 649–653.

1229 Richerol, T., Pienitz, R., Rochon, A., 2012. Modern dinoflagellate cyst assemblages in surface
1230 sediments of Nunatsiavut fjords (Labrador, Canada). Marine Micropaleontology 88, 54–64.

1231 Riding, J.B., Kyffin-Hughes, J.E., 2004. A review of the laboratory preparation of palynomorphs with a
1232 description of an effective non-acid technique. Revista Brasileira de Paleontologia 7, 13–44.

1233 Riding, J.B., Pound, M.J., Hill, T.C.B., Stukins, S., Feist-Burkhardt, S., 2012. The John Williams Index of
1234 Palaeopalynology. Palynology 36, 224–233.
1235 Robert, C., Diester-Haass, L., Paturel, J., 2005. Clay mineral assemblages, siliciclastic input and
1236 paleoproductivity at ODP Site 1085 off Southwest Africa: a Late Miocene–early Pliocene
1237 history of Orange river discharges and Benguela current activity, and their relation to global
1238 sea level change. Marine Geology 216, 221–238.
1239 Robinson, M.M., Valdes, P.J., Haywood, A.M., Dowsett, H.J., Hill, D.J., Jones, S.M., 2011. Bathymetric
1240 controls on Pliocene North Atlantic and Arctic sea surface temperature and deepwater
1241 production. Palaeogeography, Palaeoclimatology, Palaeoecology 309, 92–97.
1242 Rochon, A., Vernal, A.D., Turon, J.-L., Matthiessen, J., Head, M.J., 1999. Distribution of recent
1243 dinoflagellate cysts in surface sediments from the North Atlantic Ocean and adjacent seas in
1244 relation to sea-surface parameters. American Association of Stratigraphic Palynologists
1245 Contribution Series 35, 146 p.
1246 Ruddiman, W.F., 2010. A paleoclimatic enigma? Science 328, 838–839.
1247 Ruddiman, W.F., 2013. Tectonic uplift and climate change, Springer Science and Business Media 534
1248 p.
1249 Salzmann, U., Haywood, A., Lunt, D., Valdes, P., Hill, D., 2008. A new global biome reconstruction and
1250 data-model comparison for the middle Pliocene. Global Ecology and Biogeography 17, 432–
1251 447.
1252 Salzmann, U., Dolan, A.M., Haywood, A.M., Chan, W.-L., Voss, J., Hill, D.J., Abe-Ouchi, A., Otto-
1253 Bliesner, B., Bragg, F.J., Chandler, M.A., Contoux, C., Dowsett, H.J., Jost, A., Kamae, Y.,
1254 Lohmann, G., Lunt, D.J., Pickering, S.J., Pound, M.J., Ramstein, G., Rosenbloom, N.A., Sohl, L.,
1255 Stepanek, C., Ueda, H., Zhang, Z., 2013. Challenges in quantifying Pliocene terrestrial
1256 warming revealed by data-model discord. Nature Climate Change 3, 969–974.

1257 Saucier, F.J., Roy, F., Gilbert, D., Pellerin, P., Ritchie, H., 2003. Modeling the formation and circulation
1258 processes of water masses and sea ice in the Gulf of St. Lawrence, Canada. Journal of
1259 Geophysical Research: Oceans 108, doi: 10.1029/2000JC000686.
1260 Savin, S.M., Douglas, R.G., Stehli, F.G., 1975. Tertiary marine paleotemperatures. Geological Society
1261 of America Bulletin 86, 1499–1510.
1262 Schreck, M., Matthiessen, J., 2013. *Batiacasphaera micropapillata*: Palaeobiogeographic distribution
1263 and palaeoecological implications of a critical Neogene species complex. In: Lewis, J.M.,
1264 Marret, F., Bradley, L., (editors). Biological and Geological Perspectives of Dinoflagellates.
1265 The Micropalaeontological Society, Special Publications. Geological Society, London, 301–
1266 314.
1267 Schreck, M., Meheust, M., Stein, R., Matthiessen, J., 2013. Response of marine palynomorphs to
1268 Neogene climate cooling in the Iceland Sea (ODP Hole 907A). Marine Micropaleontology
1269 101, 49–67.
1270 Shackleton, N.J., Backman, J., Zimmerman, H., Kent, D.V., Hall, M.A., Roberts, D.G., Schnitker, D.,
1271 Baldauf, J.G., Desprairies, A., Homrighausen, R., Huddlestun, P., Keene, J.B., Kaltenback, A.J.,
1272 Krumsiek, K.A.O., et al., 1984, Oxygen Isotope Calibration of the Onset of Ice-Rafting and
1273 History of Glaciation in the North-Atlantic Region: Nature 307, 620–623.
1274 Shackleton, N.J., Kennett, J., 1975. Paleotemperature history of the Cenozoic and initiation of
1275 Antarctic glaciation: Oxygen and carbon isotope analyses in DSDP sites 277 279, and 281.
1276 Initial Reports of the Deep Sea Drilling Project 29, 743–755.
1277 Shevenell, A.E., Kennett, J.P., Lea, D.W., 2004. Middle Miocene southern ocean cooling and Antarctic
1278 cryosphere expansion. Science 305, 1766–1770.
1279 Siesser, W.G., 1980. Late Miocene origin of the Benguela upswelling system off northern Namibia.
1280 Science 208, 283–285.
1281 Sijp, W.P., Anna, S., Dijkstra, H.A., Flögel, S., Douglas, P.M., Bijl, P.K., 2014. The role of ocean
1282 gateways on cooling climate on long time scales. Global and Planetary Change 119, 1–22.

1283 Sluijs, A., Pross, J., Brinkhuis, H., 2005. From greenhouse to icehouse; organic-walled dinoflagellate
1284 cysts as paleoenvironmental indicators in the Paleogene. Earth-Science Reviews 68, 281–
1285 315.
1286 Spicer, R.A., Harris, N.B.W., Widdowson, M., Herman, A.B., Guo, S., Valdes, P.J., Wolfe, J.A., Kelley,
1287 S.P., 2003. Constant elevation of Southern Tibet over the past 15 million years. Nature 412,
1288 622-624.

1289 Stap, L. B., van de Wal, R.S.W., De Boer, B., Bintanja, R., Lourens, L.J., 2016. The MMCO-EOT
1290 conundrum: Same benthic δ18O, different CO2. Paleoceanography 31, 1270–1282.

1291 Stein, R., Fahl, K., Schreck, M., Knorr, G., Niessen, F., Forwick, M., Gebhardt, C., Jensen, L., Kaminski,
1292 M., Kopf, A., Matthiessen, J., Jokat, W., Lohmann, G., 2016. Evidence for ice-free summers in
1293 the Late Miocene central Arctic Ocean. Nature Communications 7, 11148.
1294 Steppuhn, A., Micheels, A., Geiger, G., Mosbrugger, V., 2006. Reconstructing the Late Miocene
1295 climate and oceanic heat flux using the AGCM ECHAM4 coupled to a mixed-layer ocean
1296 model with adjusted flux correction. Palaeogeography, Palaeoclimatology, Palaeoecology
1297 238, 399–423.
1298 Taylor, F.J.R., Hoppenrath, M., Saldarriaga, J.F., 2008. Dinoflagellate diversity and distribution.
1299 Biodiversity and Conservation 17, 407–418.
1300 Tzanova, A., Herbert, T.D., Peterson, L., 2015. Cooling Mediterranean Sea surface temperatures
1301 during the Late Miocene provide a climate context for evolutionary transitions in Africa and
1302 Eurasia. Earth and Planetary Science Letters 419, 71–80.

1303 Utescher, T., Bondarenko, O.V., Mosbrugger, V., 2015. The Cenozoic Cooling – continental signals
1304 from the Atlantic and Pacific side of Eurasia. Earth and Planetary Science Letters 415, 121–
1305 133.

1306 Versteegh, G.J., Blokker, P., Bogus, K.A., Harding, I.C., Lewis, J., Oltmanns, S., Rochon, A., Zonneveld,
1307 K.A., 2012. Infra red spectroscopy, flash pyrolysis, thermally assisted hydrolysis and

1308 methylation (THM) in the presence of tetramethylammonium hydroxide (TMAH) of cultured
1309 and sediment-derived *Lingulodinium polyedrum* (Dinoflagellata) cyst walls. Organic
1310 Geochemistry 43**,** 92–102.
1311 Verhoeven, K., Louwye, S., 2013. Palaeoenvironmental reconstruction and biostratigraphy with
1312 marine palynomorphs of the Plio–Pleistocene in Tjörnes, Northern Iceland.
1313 Palaeogeography, Palaeoclimatology, Palaeoecology 376, 224–243.
1314 Verleye, T.J., Louwye, S., 2010. Recent geographical distribution of organic-walled dinoflagellate
1315 cysts in the southeast Pacific (25–53 S) and their relation to the prevailing hydrographical
1316 conditions. Palaeogeography, Palaeoclimatology, Palaeoecology 298, 319–340.
1317 Versteegh, G.J., Zonneveld, K.A., 1994. Determination of (palaeo-) ecological preferences of
1318 dinoflagellates by applying detrended and canonical correspondence analysis to Late
1319 Pliocene dinoflagellate cyst assemblages of the south Italian Singa section. Review of
1320 Palaeobotany and Palynology 84, 181–199.
1321 von Hagke, C., Oncken, O., Ortner, H., Cederbom, C.E., Aichholzer, S., 2014. Late Miocene to present
1322 deformation and erosion of the Central Alps — Evidence for steady state mountain building
1323 from thermokinematic data. Tectonophysics 632, 250–260.

1324 Warny, S., Askin, R.A., Hannah, M.J., Mohr, B.A., Raine, J.I., Harwood, D.M., Florindo, F., 2009.
1325 Palynomorphs from a sediment core reveal a sudden remarkably warm Antarctica during the
1326 middle Miocene. Geology 37, 955–958.
1327 Wijnker, E., Bor, T., Wesselingh, F., Munsterman, D., Brinkhuis, H., Burger, A., Vonhof, H., Post, K.,
1328 Hoedemakers, K., Janse, A., 2008. Neogene stratigraphy of the Langenboom locality (Noord-
1329 Brabant, the Netherlands). Netherlands Journal of Geosciences-Geologie en Mijnbouw 87,
1330 165–180.
1331 Williams, G.L., Fensome, R.A. and MacRae, R.A., 2017. The Lentin and Williams index of fossil
1332 dinoflagellates. 2017 edition. American Association of Stratigraphic Palynologists
1333 Contributions Series 48, 1097 p.

1334 Williams, M., Haywood, A.M., Taylor, S.P., Valdes, P.J., Sellwood, B.W., Hillenbrand, C.-D., 2005.
1335 Evaluating the efficacy of planktonic foraminifer calcite $\delta^{18}O$ data for sea surface
1336 temperature reconstruction for the Late Miocene. Geobios 38, 843–863.
1337 Wilson, D.S., Pollard, D., Deconto, R.M., Jamieson, S.S., Luyendyk, B.P., 2013. Initiation of the West
1338 Antarctic Ice Sheet and estimates of total Antarctic ice volume in the earliest Oligocene.
1339 Geophysical Research Letters 40, 4305–4309.
1340 Woods, M.A., Vandenbroucke, T.R., Williams, M., Riding, J.B., De Schepper, S., Sabbe, K., 2014.
1341 Complex response of dinoflagellate cyst distribution patterns to cooler early Oligocene
1342 oceans. Earth-Science Reviews 138, 215–230.
1343 Wright, J.D., Miller, K.G., Fairbanks, R.G., 1992. Early and middle Miocene stable isotopes:
1344 implications for deepwater circulation and climate. Paleoceanography 7, 357–389.
1345 You, Y., Huber, M., Müller, R., Poulsen, C., Ribbe, J., 2009. Simulation of the middle Miocene climate
1346 optimum. Geophysical Research Letters 36, doi: 10.1029/2008GL036571.
1347 Zachos, J., Pagani, M., Sloan, L., Thomas, E., Billups, K., 2001. Trends, rhythms, and aberrations in
1348 global climate 65 Ma to present. Science 292, 686–693.
1349 Zachos, J.C., Dickens, G.R., Zeebe, R.E., 2008. An early Cenozoic perspective on greenhouse warming
1350 and carbon-cycle dynamics. Nature 451, 279–283.
1351 Zhang, Y.G., Pagani, M., Liu, Z., Bohaty, S.M., DeConto, R., 2013. A 40-million-year history of
1352 atmospheric CO_2. Philosophical Transactions of the Royal Society of London A:
1353 Mathematical, Physical and Engineering Sciences 371.
1354 Zonneveld, K.A., Brummer, G.A., 2000. (Palaeo-) ecological significance, transport and preservation
1355 of organic-walled dinoflagellate cysts in the Somali Basin, NW Arabian Sea. Deep Sea
1356 Research Part II: Topical Studies in Oceanography 47, 2229–2256.
1357 Zonneveld, K.A., Marret, F., Versteegh, G. J., Bogus, K., Bonnet, S., Bouimetarhan, I., Crouch, E., de
1358 Vernal, A., Elshanawany, R., Edwards, L., 2013a. Atlas of modern dinoflagellate cyst
1359 distribution based on 2405 data points. Review of Palaeobotany and Palynology 191, 1–197.

1360 Zonneveld, K.A., Versteegh, G.J., De Lange, G.J., 1997. Preservation of organic-walled dinoflagellate
1361 cysts in different oxygen regimes: a 10,000 year natural experiment. Marine
1362 Micropaleontology 29, 393–405.
1363 Zonneveld, K.A.F.; Versteegh, G.J.M., De Lange, G.J., 2001. Palaeoproductivity and post-depositional
1364 aerobic organic matter decay reflected by dinoflagellate cyst assemblages of the Eastern
1365 Mediterranean S1 sapropel. Marine Geology, 172, 181–195.
1366 Zonneveld, K.A.F., Marret, F., Versteegh, G.J., Bogus, K., Bonnet, S., Bouimetarhan, I., Crouch, E., De
1367 Vernal, A., Elshanawany, R., Edwards, L., Esper, O., Forke, S., Grøsfjeld, K., Henry, M.,
1368 Holzwarth, U., Kielt, J.-F., Kim, S.-Y., Ladouceur, S., Ledu, D., Chen, L., Limoges, A., Londeix, L.,
1369 Lu, S.-H., Mahmoud, M.S., Marino, G., Matsouka, K., Matthiessen, J., Mildenhall, D.C.,
1370 Mudie, P.J., Neil, H.L., Pospelova, V., Qi, Y., Radi, T., Richerol, T., Rochon, A., Sangiorgi, F.,
1371 Solignac, S., Turon, J.-L., Verleye, T., Wang, Y., Wang, Z., Young, M., 2013b. Geographic
1372 distribution of dinoflagellate cysts in surface sediments, doi: 10.1594/PANGAEA.818280
1373